Molecular Therapy
Original Article

HucMSC-Derived Exosomes Mitigate the Age-Related Retardation of Fertility in Female Mice

Weijie Yang,[1,2,6] Jing Zhang,[1,6] Boqun Xu,[3,6] Yuanlin He,[1] Wei Liu,[1] Jiazhao Li,[1] Songying Zhang,[2] Xiaona Lin,[2] Dongming Su,[4] Tinghe Wu,[5] and Jing Li[1]

[1]State Key Laboratory of Reproductive Medicine, Nanjing Medical University, Nanjing 210029, China; [2]Assisted Reproduction Unit, Department of Obstetrics and Gynecology, Sir Run Run Shaw Hospital, Zhejiang University School of Medicine, Key Laboratory of Reproductive Dysfunction Management of Zhejiang Province, Hangzhou 310016, China; [3]Department of Obstetrics and Gynecology, The Second Affiliated Hospital of Nanjing Medical University, Nanjing 210029, China; [4]Centre of Pathology and Clinical Laboratory, Sir Run Run Hospital, Nanjing Medical University, Nanjing 210029, China; [5]Department of Biotechnology and Biomedicine, Yangtze Delta Region Institutes of Tsinghua University, Jiaxing 314006, China

In mammals, resting primordial follicles serve as the ovarian reserve. The decline in ovarian function with aging is characterized by a gradual decrease in both the quantity and quality of the oocytes residing within the primordial follicles. Many reports show that mesenchymal stem cells have the ability to recover ovarian function in premature ovarian insufficiency (POI) or natural aging animal models; however, the underlying mechanism remains unclear. In this study, using exosomes derived from human umbilical cord mesenchymal stem cells (HucMSC-exos), we found the specific accumulation of exosomes in primordial oocytes. The stimulating effects of exosomes on primordial follicles were manifested as the activation of the oocyte phosphatidylinositol 3-kinase (PI3K)/mTOR signaling pathway and the acceleration of follicular development after kidney capsule transplantation. Further analysis revealed the stimulatory effects of HucMSC-exos on primordial follicles were through carrying functional microRNAs, such as miR-146a-5p or miR-21-5p. In aged female mice, the intrabursal injection of HucMSC-exos demonstrated the recovery of decreased fertility with increased oocyte production and improved oocyte quality. Although assisted reproductive technologies have been widely used to treat infertility, their overall success rates remain low, especially for women in advanced maternal age. We propose HucMSC-exos as a new approach to mitigate the age-related retardation of fertility in women.

INTRODUCTION

It is generally accepted that in mammals, oocytes cannot renew themselves postnatally or during the adult life and that the number of oocytes is already fixed as primordial follicles formed before or around birth.[1] To maintain this "reserve" and provide a steady supply of fertilizable oocytes during the reproductive lifespan, primordial follicles must remain quiescent, sometimes for decades, until being activated for growth via a highly controlled mechanism.[2,3] The constant demise of primordial follicles and the continuous recruitment of primordial follicles over time depletes the ovarian reserve, leading to menopause, which occurs in humans at approximately 50 years of age when less than 1,000 primordial follicles remain in the ovary.[4] In reality, ovarian aging occurs earlier, before menopause. According to what is known about the human female biological clock, a woman's fertility begins to decline significantly in her early 30s, with a steep decrease beginning after the age of 35.[5] The aging process is thought to be associated with gradual decreases in both the quantity and quality of the oocytes residing within the primordial follicles of the ovarian cortex.[6,7] In pathological conditions, premature ovarian insufficiency (POI) occurs in 1%–4% of women, which is characterized by the absence of normal ovarian function due to the early depletion of the primordial follicle pool before the age of 40.[8] For such a significant reduction or even depletion of the ovarian reserve, assisted reproduction can help only to a limited extent, leaving many couples childless after prolonged infertility therapy.[5] Thus, manipulating these dormant follicles in the ovary may represent a paradigm shift for women who are undergoing natural or premature ovarian aging.

During the past few years, mesenchymal stem cells (MSCs) have attracted great attention due to their large therapeutic potential. As one type of multipotent stem cell, the MSC can be derived from adipose tissue, bone, the umbilical cord, the placenta, amniotic fluid, and the connective tissue of most organs.[9] Human umbilical cord MSCs (HucMSCs), in contrast to other MSC types from other sources, have become a prominent stem cell type used for allogeneic cell-based therapy because of their advantages in terms of ethical access, abundant tissue source, low immunogenicity, and rapid renewal properties.[10] To

Received 15 March 2019; accepted 4 February 2020;
https://doi.org/10.1016/j.ymthe.2020.02.003.

[6]These authors contributed equally to this work.

Correspondence: Jing Li, State Key Laboratory of Reproductive Medicine, Nanjing Medical University, Xuehai Building, Room B101, 818 Tianyuandonglu, Nanjing, Jiangsu 210029, China.
E-mail: ljwth@njmu.edu.cn

Please cite this article in press as: Yang et al., HucMSC-Derived Exosomes Mitigate the Age-Related Retardation of Fertility in Female Mice, Molecular Therapy (2020), https://doi.org/10.1016/j.ymthe.2020.02.003

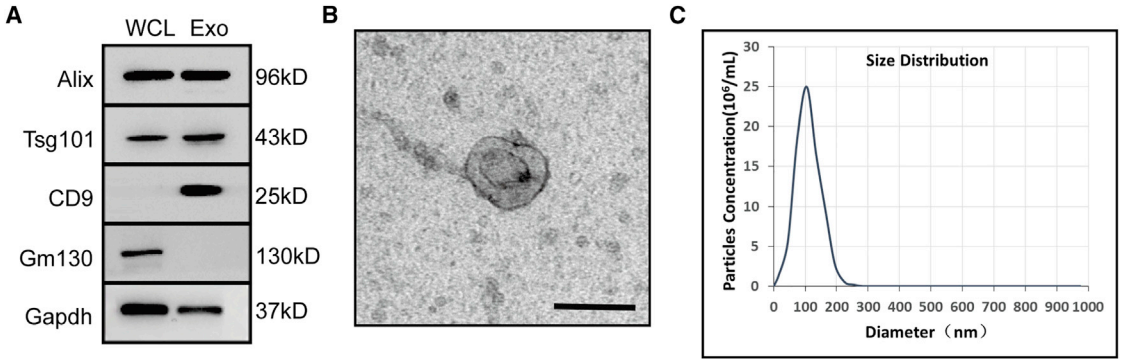

Figure 1. Characterization of HucMSC-exos

(A) Western blot analysis of exosome-related markers Alix, Tsg101, and CD9. Plasma protein Gm130 was used as a negative control. Both lanes were loaded with 20 μg of proteins as measured by Qubit 3.0. WCL, whole-cell lysate; Exo, exosome. (B) Representative image of HucMSC-exos observed by transmission electron microscope (TEM). Scale bar, 100 μm. (C) Nanoparticle tracking analysis of size distribution and concentration of HucMSC-exos. The mean protein concentration and mean particle concentration of the HucMSC-exos were 0.79 mg/mL and 2.7 × 10^{10} particles/mL, respectively.

date, HucMSCs have been under investigation in a variety of clinical therapeutic trials. The application areas include various conditions, such as neurological deficits, liver diseases, immune system diseases, diabetes, and acute leukemia.[11] MSCs have also been proven to be effective toward recovering ovarian function and improving fertility in POI or natural aging animal models.[12–14] Recently, a successful clinical pregnancy was reported via the transplantation of collagen/HucMSCs into the ovaries of POI patients.[15] Despite the therapeutic effect observed, however, the underlying molecular mechanism, especially how the ovarian reserve is regulated, remains unknown.

In addition to the increased use of MSC transplantation in the clinic, many studies have reported that MSC proliferation at the site of engraftment and subsequent differentiation into appropriate cell types are rare.[16] The therapeutic efficacy of engrafted MSCs is also not dependent on the physical contacts between MSCs and local tissue cells.[17] Many researchers think that MSCs function through their secreted products, more specifically, exosomes (exos).[16] Exos are a type of extracellular vesicle (EV) of endosomal origin that is 40–150 nm in size, and exos play important roles in intercellular communication by delivering microRNAs (miRNAs), mRNAs, and proteins to recipient cells.[18] Similar to their cell source, MSC-derived exos help to maintain tissue homeostasis and enable the recovery of critical cellular functions by initiating the process of repair and regeneration.[19] Thus, instead of stem cell transplantation therapy, MSC-exos may be a better choice in the clinic because of their advantages in terms of low immunogenicity, lack of tumorigenicity, high clinical safety, and low ethical risk.[17,20] They have been shown to have intrinsic therapeutic effects on an increasingly wide spectrum of diseases via their involvement in various biological processes, such as wound healing, inflammation, hypertension, cardiovascular disease, brain injury, and cancers.[21] Two recent studies have reported that MSC-exos can repair chemotherapy-induced ovarian damage in mouse models. Although the molecular mechanisms are different, both studies highlight the regulatory effects of exos on the proliferation and apoptosis of granulosa cells.[22,23] Until now, whether MSC-derived exos function in regulating the primordial follicle pool remains unclear, as do the underlying mechanisms.

In this study, we demonstrated the stimulatory effects of HucMSC-derived exos on primordial follicles through the activation of the phosphatidylinositol 3-kinase (PI3K)/mTOR signaling pathway in oocytes. When HucMSC-exos were intrabursally injected into aged female mice, they showed similar effects on the ovarian reserve, together with a significant improvement in oocyte quality. Based on the improvements brought about by HucMSC-exo treatment in terms of oocyte production and quality in aged mice, we propose that HucMSC-exos may represent a new approach toward enhancing decreased fertility in women with a diminished ovarian reserve.

RESULTS

Characterization of HucMSC-exos

EVs were isolated from conditional media of passage 3–7 HucMSCs. The identity and purity of the nanoparticles were determined by western blot, TEM (transmission electron microscopy), and nanoparticle tracking analysis (NTA). Western blotting showed that the EVs were enriched with exosomal surface markers Alix, Tsg101, and CD9 but were negative for the expression of Gm130, a cytoplasmic Golgi complex marker (Figure 1A).[24] By TEM, these nanoparticles exhibited a typical round-cup-like exosome structure that was approximately 100 nm in size (Figure 1B). The particle size distribution and particle pictorial diagram of the EVs were also recorded by NTA, and the particles had a typical modal size of 62.7–146.1 nm (Figure 1C). Thus, these nanoparticles were actually exos from HucMSCs (HucMSC-exos).

Specific Enrichment of HucMSC-exos in Oocytes of Primordial Follicles

To observe the uptake of exos by tissues cultured *in vitro*, HucMSC-exos were first labeled with PKH67 dye and incubated with ovaries from newborn mice for indicated times (0, 3, 6, 12, and 24 h). Newborn ovaries at postnatal day (P)2.5 contain mainly primordial

Please cite this article in press as: Yang et al., HucMSC-Derived Exosomes Mitigate the Age-Related Retardation of Fertility in Female Mice, Molecular Therapy (2020), https://doi.org/10.1016/j.ymthe.2020.02.003

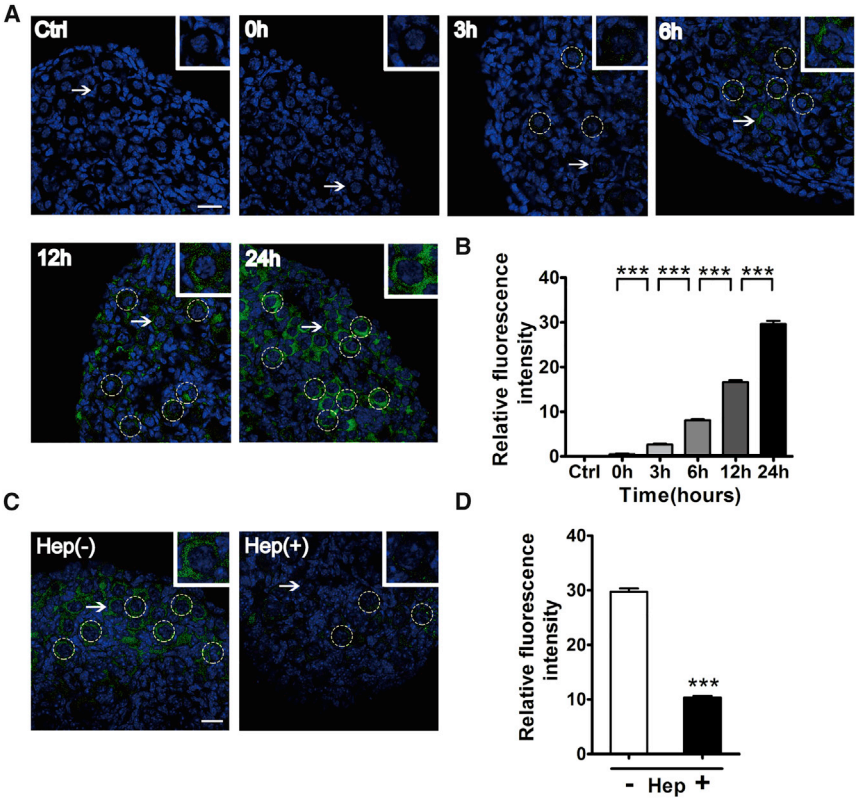

Figure 2. Uptake of HucMSC-exos by Cultured Newborn Ovaries

Newborn ovaries (P2.5) were incubated with PKH67-labeled exos for 0, 3, 6, 12, and 24 h. (A) Gradual accumulation of HucMSC-exos in primordial follicles. Ovaries were collected for frozen sections and nuclei were stained with Hoechst 33342. Green indicates exos; blue shows Hoechst 33342. For the control (Ctrl), ovaries were incubated with PBS for 24 h. (B) Fluorescence intensity analysis of labeled HucMSC-exos. n = 4/group. (C) Internalization of HucMSC-exos after ovaries were cultured for 24 h in the presence (left panel) or absence (right panel) of 5,000 IU of heparin (Hep). (D) Fluorescence intensity analysis of internalized HucMSC-exos. n = 4/group. Insets represent magnification of representative primordial follicles marked by white arrows. Dotted circles indicate primordial follicles. Data are shown as mean ± SEM. ***$p < 0.001$. Scale bars, 20 μm.

follicles and are good resources to study the process of follicular activation.[25] As shown in Figures 2A and 2B, with the extending of the culture time, compared to other cell types in the ovary, PKH67-labeled exos began to accumulate in the oocytes, and the fluorescence intensity increased gradually, with the highest level observed at 24 h of treatment. Exos have been reported to depend on cell-surface heparan sulfate proteoglycans for their internalization.[26] Ovaries were also treated with heparin (5,000 IU/mL) and exos together, and the results showed that heparin could effectively block the uptake of exos into primordial oocytes (Figures 2C and 2D).

HucMSC-exos Promote Follicular Activation and Development in Newborn Mice

Stimulation of both PI3K and mTOR signaling pathways in oocytes has been proven to be essential for the activation of primordial follicles.[3] To study the effects of HucMSC-exos on primordial follicles, we incubated newborn ovaries with different doses of HucMSC-exos for 24 h. Ovaries without any treatment or ovaries co-cultured with HucMSCs were used as a negative or positive control, respectively (Figure S1A). The western blot results showed a strongly increased level of phosphorylated Akt, indicating activation of PI3K signaling, and increased levels of phosphorylated mTOR and rpS6, indicating activated mTORs signaling (p-Akt, p-mTOR, p-rpS6) in exo-treated ovaries in a dose-dependent manner (Figure 3A). Immunostaining of Foxo3a, a downstream inhibitory transcriptional factor of the PI3K signaling pathway that labels activated oocytes by translocation from the oocyte nucleus to the cytoplasm, also revealed an increased number of activated primordial follicles (~20%) in the exo-treated group at 20 μg/mL HucMSC-exos (Figures 3B and 3C).[25] Newborn ovaries were then treated with HucMSC-exos with/without the PI3K inhibitor LY294002, the Akt inhibitor Akt VIII, the mTOR inhibitor rapamycin, or the exo-uptake inhibitor heparin. We found the exo-induced activation of PI3K and mTOR signals could be effectively blocked by heparin and all of the other inhibitors (Figure 3D). In another experiment, after finishing the above treatment, ovaries in each group were transferred into control media for 96 h to follow ovarian development. As expected, the best follicular development was observed in exo-treated ovaries, with more developed follicles (from primary to secondary follicles) in the center of the ovary. However, in the inhibitor-treated ovaries, most follicles remained at the primordial follicle stage and seldom developed into secondary follicles (Figure 3E). To see the specific stimulation of HucMSC-exos on the oocyte PI3K/mTOR signaling pathway, we separated primordial oocytes from newborn ovaries and incubated them with HucMSC-exos with/without the mentioned inhibitors. As shown in Figure S1B, similar blocking effects were found in inhibitor co-treated groups. Meanwhile, knockdown experiments were performed on newborn ovaries with chemically modified mTOR small interfering RNAs (siRNAs). The result revealed the failure of HucMSC-exos to activate the PI3K/mTOR signaling pathway in treated ovaries, which was shown by the decreased phosphorylation of mTOR, rpS6, and Akt (Figures S1C and S1D) as compared with the control group. Thus, the results suggest the specificity of exo treatment on the oocyte PI3K/mTOR signaling pathway in regulating the activation of primordial follicles.

To further evaluate the effects of HucMSC-exos on follicular growth and development, paired ovaries were separated and treated with or without exos for 24 h, followed by transplantation under the kidney capsules of the same ovariectomized adult recipient.[27] We first

Please cite this article in press as: Yang et al., HucMSC-Derived Exosomes Mitigate the Age-Related Retardation of Fertility in Female Mice, Molecular Therapy (2020), https://doi.org/10.1016/j.ymthe.2020.02.003

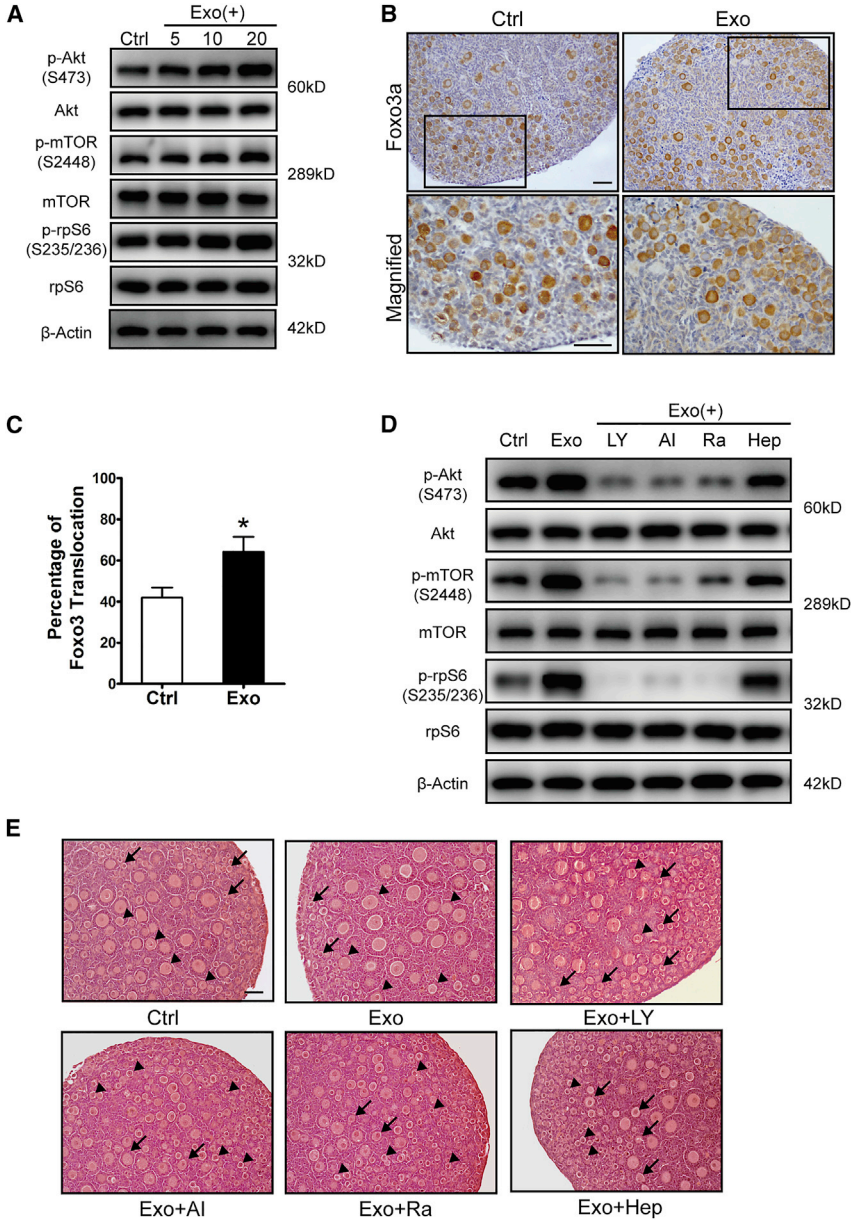

Figure 3. Activation of Primordial Follicles after HucMSC-exo Treatment

Newborn ovaries were treated for 24 h with HucMSC-exos at 5, 10, or 20 μg/mL (3×10^8, 6×10^8, 1.2×10^9 particles/mL, respectively). (A) Dose-dependent activation of the PI3K-Akt-mTOR signaling pathway in ovaries with increased expression of p-AKT (Ser473), p-mTOR (Ser2448), and p-rpS6 (Ser235/236). The expression of rpS6, mTOR, and β-tubulin were used as internal controls. (B) Immunostaining of Foxo3a in primordial follicles after newborn ovaries were incubated with 20 μg/mL HucMSC-exos for 24 h. The lower panel represents the magnified images of black frames in the upper panel. (C) Percentage of activated primordial follicles with nucleus exclusion of Foxo3a in control and exo-treated ovaries. n = 3/group. (D) Blockage of the PI3K-Akt-mTOR signaling pathway by its specific inhibitors LY294002, Akt VIII, and rapamycin and the exosome internalization inhibitor heparin. LY, LY294002; AI, Akt VIII; Ra, rapamycin; Hep, heparin. (E) Histology of ovaries collected at 96 h in each group. After 24 h of treatment, ovaries in each group were further cultured in control media for 72 h. Arrowhead indicates primordial follicles, and arrow indicates activated follicles. Data are shown as mean ± SEM. *$p < 0.05$. Scale bars, 50 μm.

collected ovaries after 48 h of transplantation. Although detection of apoptosis by TUNEL (terminal deoxynucleotidyltransferase-mediated deoxyuridine triphosphate nick end labeling) assay was seldomly found between paired ovaries, PCNA (proliferating cell nuclear antigen) staining showed increased positive signals in nuclei of oocytes or granulosa cells in exo-treated ovaries (Figures S1E and S1F). After 14 days of engraftment, the ovaries were collected; the ovarian volume and weight after exo treatment were greater than those of the control non-treated ovaries (Figures 4A and 4B). Histological analysis further revealed accelerated follicular development, with more large antral follicles being observed in the exo-treated ovaries (Figure 4C). After counting follicles by means of serial sections, we found significant decreases in the numbers of primordial follicles and increases in the numbers of growing follicles at different developmental stages in the exo-treated ovaries, in which the percentage of large antral follicles increased nearly 2-fold relative to the controls (Figure 4D). Moreover, real-time qPCR results indicated higher expression of the oocyte development-related genes *Gdf9* and *Bmp15*, granulosa cell-associated genes *Amhr2* and *Kitl*, and gonad steroid synthesis-related genes *Fshr* and *Star* in the exo-treated ovaries (Figure 4E).[28] We also checked the expression of Cx37, a key gap junction protein that coordinated communications between oocyte and cumulous granulosa cells in follicular development, in collected ovarian samples.[29] As shown in Figure 4F, discrete punctate spots of Cx37 staining, close to or at the oocyte membrane, could be clearly observed in exo-treated ovaries, whereas such typical Cx37 stainings were hardly seen in control ovaries. Similarly, western blot also showed increased expressions of Cx37 in treated ovaries (Figure 4G).

We then isolated germinal vesicle (GV) oocytes or mature metaphase II (MII) oocytes (*in vivo* matured [IVO]) from the HucMSC-exo-treated ovaries for *in vitro* maturation (IVM) or *in vitro* fertilization (IVF), respectively, at 18 days after transplantation to evaluate their developmental potential. The IVM results showed similar percentages of oocyte maturation to those from superovulated ovaries without transplantation (normal control) (Figures 5A and 5D). Immunofluorescence of β-tubulin in mature oocytes from both IVM and IVO also

Please cite this article in press as: Yang et al., HucMSC-Derived Exosomes Mitigate the Age-Related Retardation of Fertility in Female Mice, Molecular Therapy (2020), https://doi.org/10.1016/j.ymthe.2020.02.003

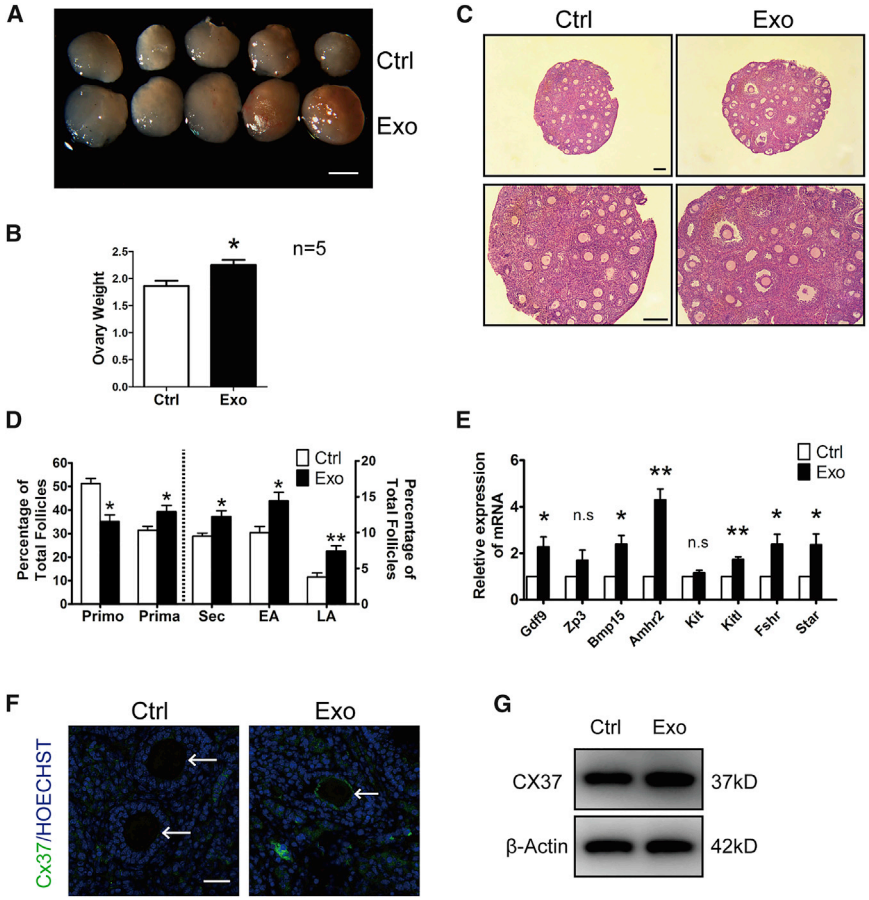

Figure 4. Acceleration of Follicular Development after HucMSC-exo Treatment

Paired ovaries were treated with or without HucMSC-exos for 24 h and transplanted into kidney capsules of the same recipient by ovariectomy. (A) Ovaries at 14 days after transplantation. Isolated ovaries from control (Ctrl) versus HucMSC-exos (Exo) treatment. Scale bar, 1 mm. (B) Comparison of ovarian weight between control and exo-treated ovaries (n = 5). (C) Ovarian histology showing more antral follicles in HucMSC-exo-treated ovaries. Scale bar, 50 μm. (D) Distribution of different stages of follicles with or without exposure to HucMSC-exos. Primo, primordial follicle; Prima. primary follicle; Sec, secondary follicle; EA, early antral follicle; LA, late antral follicle. n = 5/group. (E) Relative expression of follicular growth and development-related genes in ovaries of each group. The levels of all tested mRNAs in control group were set to 1. n = 3/group. (F) Immunofluorescence of Cx37 in ovaries treated with or without HucMSC-exos. Arrows point to oocytes. Green represents Cx37; blue represents Hoechst 33342. Scale bar, 20 μm. (G) Western blot of Cx37 expressions in ovaries treated with or without HucMSC-exos. The expression of β-actin was used as an internal control. Data are shown as mean ± SEM. *$p < 0.05$, **$p < 0.01$.

revealed normal spindle distributions and low percentages of oocytes with aberrant spindles (Figures 5B, 5C, and 5E). After IVF using donor sperm, mature oocytes from exo-treated ovaries developed from two-cell embryos to blastocysts after 96 h of culture (Figure 5F), and comparable embryonic development was observed as in the normal control group (Figure 5G). Therefore, the internalization of HucMSC-exos in newborn ovaries can dramatically promote follicular development without any side effects on oocyte maturation, fertilization, or early embryonic development.

HucMSC-exo-Specific MicroRNAs Function in Regulating Follicular Activation of Newborn Mice

As one of the most vital components in MSC-exos, exo-miRNAs have been reported to mediate intercellular communications and promote target cellular functions in various tissues.[30,31] To elucidate the underlining mechanism of HucMSC-exos on primordial follicles, we first considered reported HucMSC-specific miRNAs as candidates, and one miRNA, miR-146a-5p, was finally chosen for further analysis because of its involvement in mediating a series of therapeutic effects of HucMSCs and its potential regulation on the PI3K signaling pathway.[32,33] Additionally, another HucMSC-enriched miRNA, miR-21-5p, was used as a positive control whose overexpression in MSCs has been reported to improve ovarian structure and function in rats with chemotherapy-induced ovarian damage through targeting PTEN (phosphatase and tensin homolog deleted on chromosome 10), an inhibitor of the PI3K signaling pathway.[34] As shown in Figure 6A, we found a significant increase of miRNA-146a-5p and miR-21-5p in HucMSC-exo-treated ovaries. However, when exos were pretreated with Antagomir-146a (ExoKd1) or Antagomir-21 (ExoKd2), such an increase was completely blocked, and the addition of miRNA mimics Agomir-146a and Agomir-21 could restore their expressions to some extent. Western blot results also showed the failure to activate the PI3K/mTOR signaling pathway in the ExoKd1 group (Figure 6B). Paired ovaries under different treatments were then used for kidney capsule transplantation to evaluate the effects of Antagomirs on primordial follicle activation and development. As compared with HucMSC-exo-treated ovaries, the results revealed decreased ovarian sizes after incubating with exos pretreated with each Antagomir (Exo versus ExoKd1 and Exo versus ExoKd2; Figure 6C). No synergistic inhibitory effects were observed when two Antagomirs were used together, suggesting that similar molecular mechanisms existed in regulating follicular activation (Exo versus Exo containing both Antagomirs [KdMix], Figure 6C). Moreover, co-treatment with Agomir-146a on ovaries cultured with miR-146a knockdown exos could increase ovarian size again (ExoKd1 versus ExoKd1+Ago 146, Figure 6C). Ovaries incubated directly with Antagomir-146a (Anta 146) or Agomir-146a (Ago 146) served as controls, and the results revealed the inhibitory or stimulatory effects on ovarian development when compared with non-treated ovaries (Figure 6C). Paired ovaries

Please cite this article in press as: Yang et al., HucMSC-Derived Exosomes Mitigate the Age-Related Retardation of Fertility in Female Mice, Molecular Therapy (2020), https://doi.org/10.1016/j.ymthe.2020.02.003

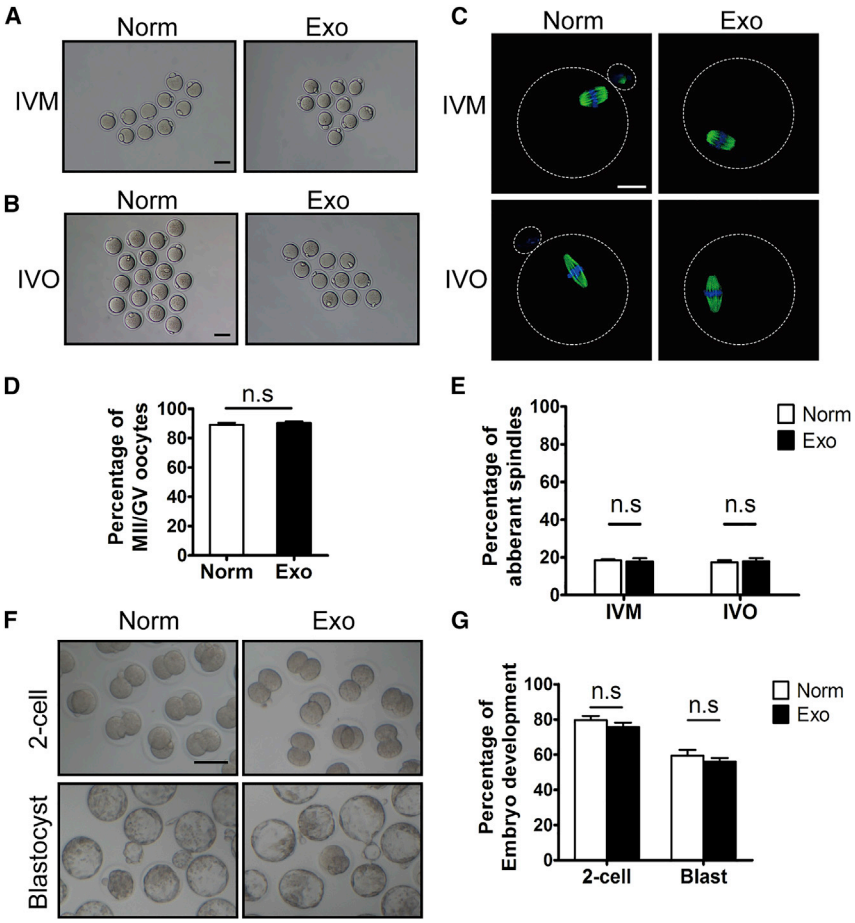

Figure 5. Evaluation of Oocyte Quality by *In Vitro* Maturation (IVM), *In Vitro* Fertilization (IVF), and Early Embryonic Development

Newborn ovaries (P2.5) treated with HucMSC-exos were transplanted into the kidney capsules of recipient mice for 18 days. GV oocytes for IVM were collected by directly puncturing fully grown follicles under the microscope, and mature MII oocytes were retrieved after a single injection of hCG into recipient mice (IVO). (A and B) Morphology of MII oocytes after IVM (A) and IVO (B). Oocytes from superovulated ovaries of 3-week-old mice were used as normal controls (Norm). (C) Immunofluorescence of β-tubulin on spindle of MII oocytes. Green indicates β-tubulin; blue indicates nuclear staining with Hoechst 33342. (D and E) Percentages of MII oocytes with aberrant spindles after IVM (D) and IVO (E) treatment. (F) Representative two-cell embryos and blastocysts after IVO oocytes being fertilized *in vitro* (IVF). (G) Efficiency of early embryonic development. Percentage of IVO mature oocytes in control and exo-treated group capable of developing into two-cell embryos and blastocysts. All experiments were performed with at least three replicates. Data are shown as mean ± SEM. n.s., not significant; *$p < 0.05$. White scale bar, 20 μm; black scale bar, 50 μm.

from the Exo versus ExoKd1 group and ExoKd1 versus Exo Kd1+Ago 146 group were then collected for morphological analysis with follicle counts. The results showed the decreased percentage of growing follicles (secondary, early, and late antral follicles) in ExoKd1-treated ovaries (Exo versus ExoKd1), and the decrease could be rescued when Ago 146 was added together (ExoKd1 versus ExoKd1+Ago146) (Figures 6D and 6E). Taken together, our results suggest the specific regulation of exo-carrying miRNAs on follicular activation and development.

HucMSC-exos Improve Fertility in Old Female Mice

Because natural ovarian aging is also characterized by minimal ovarian reserve, we selected mice at 10 months of age and injected HucMSC-exos into the unilateral ovarian bursa to determine whether the stimulatory effects on primordial follicles still existed (Figure 7A). Three weeks later, the paired ovaries were collected for histological analysis, and the results showed more growing follicles in the exo-treated lateral ovaries (Figure S2). Follicle counts of continuous ovarian tissue sections verified the stimulatory effects of HucMSC-exos on follicular development, with a decreased percentage of primordial follicles and a significantly increased percentage of large antral follicles (Figure 7B). We next divided the mice into two groups: the control group was injected with PBS, and the treated group was injected with exos into the bursas bilaterally (Figure 7A). Three weeks later, the mice in the two groups were mated with adult male mice for 4 months to evaluate the fertility of these older mice. When the fertility test was complete, the female mice in the two groups were housed for another 2 weeks to exclude undetected pregnancies, and the non-pregnant mice were used for oocyte collection through superovulation. As shown in Figure 7C, during the mating trials, only four mice in the control group (n = 15 in each group) delivered pups, whereas nine mice in the treated group had deliveries. Moreover, although the mice in both groups showed decreased fertility, the delivered pup number per female in the HucMSC-exo-treated group was 2-fold that of the control mice (4.5 versus 2 pups per female) (Figure 7D). Thus, regardless of the number of mothers with deliveries or the average number of delivered pups, exo treatment provided solid enhancement of fertility in older females.

Finally, oocytes were collected from the control- and HucMSC-exo-treated mice for oocyte quality analysis. As shown in Figures 8A and 8B, nearly 40% of the ovulated oocytes in control mice had abnormal spindle morphology, whereas the percentage decreased to 20% in the treated mice. The results suggested that HucMSC-exos treatment could rescue age-related meiosis abnormalities to some extent. In mammals, the decline in oocyte quality is related to abnormalities in mitochondrial functions. Alterations in the oxidative stress level (reactive oxygen species [ROS]) and mitochondrial membrane potential ($\Delta\Psi m$) are good indexes to reflect mitochondrial

Please cite this article in press as: Yang et al., HucMSC-Derived Exosomes Mitigate the Age-Related Retardation of Fertility in Female Mice, Molecular Therapy (2020), https://doi.org/10.1016/j.ymthe.2020.02.003

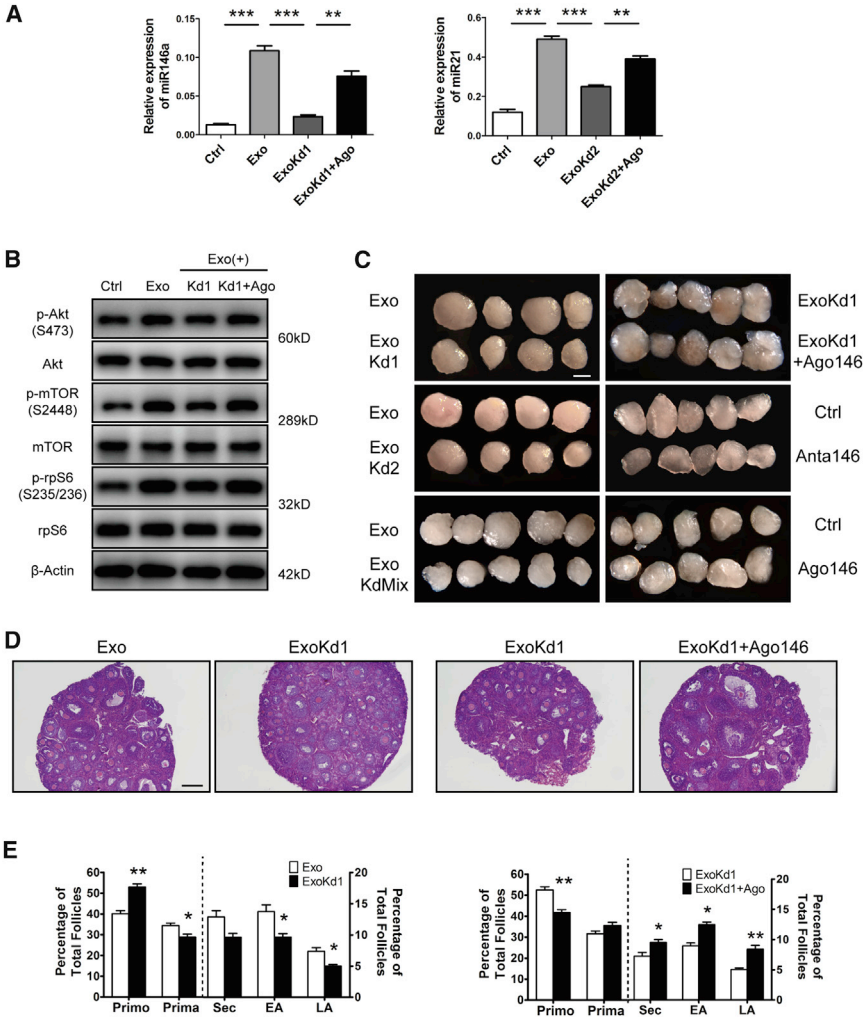

Figure 6. Effects of Exo-Carrying MicroRNAs on Follicular Activation and Development

(A) Expression of miR-146a-5p and miR-21-5p in ovaries after 24 h of different treatments. Crtl, control (PBS); Exo, HucMSC-exos (20 μg/mL); ExoKd1, exos carrying Antagomir-146a-5p; ExoKd2, exos carrying Antagomir-21-5p; ExoKd1+Ago, Agomir-146a-5p; ExoKd2+Ago, Agomir-21-5p. (B) Ovarian expression of p-Akt (Ser473), p-mTOR (Ser2448), and p-rpS6 (Ser235/236) after 24 h of treatments. The expressions of Akt, mTOR, rpS6, and β-actin were used as internal controls. (C) Comparisons of ovarian development after various treatment combinations. Paired ovaries (P2.5) were separated for different treatments with 24-h incubation and then were transplanted under kidney capsules of recipient mice for 14 days. Exo KdMix, exos containing both Antagomirs; Anta 146, Antagomir-146a-5p; Ago 146, Agomir-146a-5p. Scale bar, 1 mm. (D) Ovarian histology between paired ovaries. Left, Exo versus ExoKd1; Right, ExoKd1 versus ExoKd1+Ago 146. Scale bar, 50 μm. (E) Distribution of different stages of follicles in paired ovaries with treatments corresponding to (D). n = 5/group. *p < 0.05, **p < 0.01, ***p < 0.001.

functions and have been shown to be related to the decline in oocyte quality during ovarian aging.[35–37] Similar to what was observed previously, we found stronger ROS staining in oocytes collected from the control mice, but the ROS levels decreased significantly in the HucMSC-exo-treated oocytes (Figures 8C and 8D). Additionally, $\Delta\Psi m$ as measured through a ratio metric analysis of JC-1 staining also showed a higher $\Delta\Psi m$ in the HucMSC-exo-treated oocytes (Figures 8E and 8F). Taken together, these results demonstrated the promotional effects of HucMSC-exos treatment on follicular development and oocyte quality in aged female mice.

DISCUSSION

Due in part to developments in the understanding of the paracrine effects of stem cell therapy, stem cell therapy has been mechanistically linked to the inherited, specific functions of secreted exos.[38] Indeed, many studies have revealed that MSC-derived exos can function as potently as parental cells in promoting regeneration and functional recovery in experimental animal models.[39–42] In this study, we demonstrated the specific stimulatory effects of HucMSC-exos on primordial follicles in cultured newborn ovaries. Further study revealed that these effects occurred through the activation of the PI3K/mTOR signaling pathway. It has long been accepted that primordial follicles are under constant inhibitory influences until they are activated by either decreases in the levels of these inhibitory factors or increases in stimulatory factors.[43] During the past few decades, studies involving transgenic mouse models have demonstrated that a key pathway in oocytes, namely, the PI3K signaling pathway, plays a crucial integrative role in regulating the balance between follicle growth suppression and activation and the maintenance of healthy quiescence. Oocyte-specific deletions of both Pten, a negative regulator of PI3K, and of Foxo3a, an inhibitory downstream transcriptional factor, lead to the overgrowth of all primordial follicles, which results in early follicular depletion in young adulthood.[44,45] In contrast to the traditional model that Tsc/mTORC1 signaling is downstream of PI3K signaling in some cell types, the two signaling pathways appear to regulate follicular activation in a synergistic and collaborative way. Although oocyte deletion of Tsc1 (hamartin), the suppressor gene of mTORC1, is also essential to activate primordial follicles, the double deletion of Tsc1 and Pten in mice leads to further synergistic enhancement of oocyte growth compared to single mutations in mice.[46] In this study, after 24 h of incubation with HucMSC-exos, both the PI3K and mTOR signaling pathways were activated in a dose-dependent manner, as shown by the significantly increased levels of phosphorylated Akt, mTOR, and rpS6. Moreover, these stimulatory effects were completely blocked by pretreatment with the PI3K inhibitor LY294002, Akt VIII, and the mTORC1 inhibitor

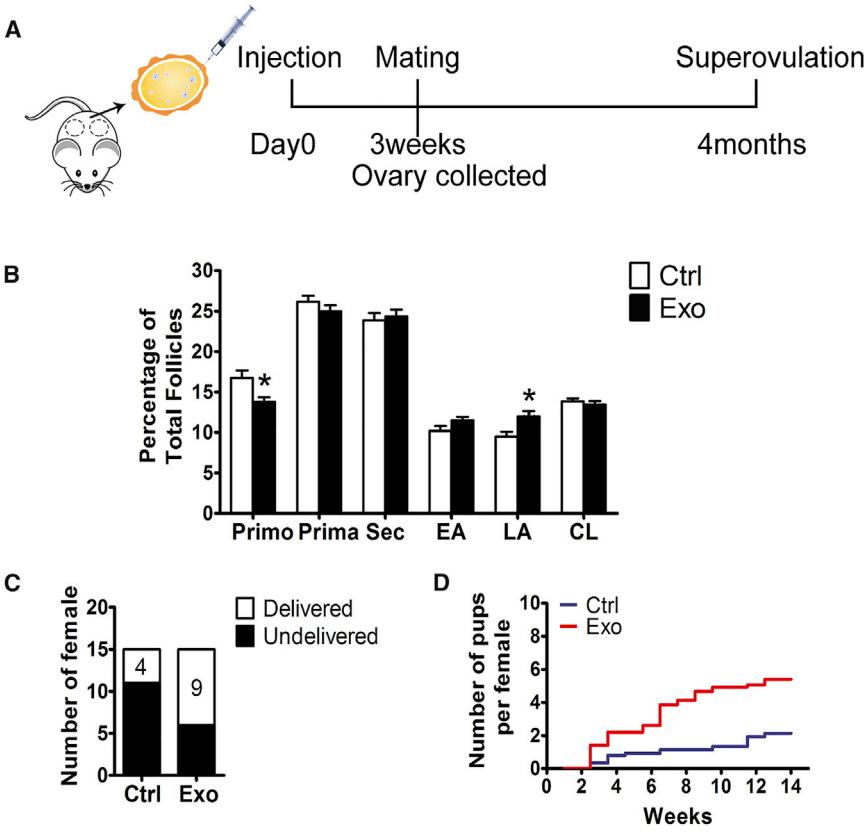

Figure 7. Stimulation of Follicular Development in Old Mice by HucMSC-exos

(A) Timeline of HucMSC-exos treatment. Mice at 10 months of age were intrabursally injected with 20 μL of HucMSC-exos or the same volume of PBS. For some mice, one lateral ovary was given HucMSC-exos and the other one received PBS. Ovaries were collected for morphology 3 weeks later. Some mice were injected with HucMSC-exos or PBS bilaterally for a 4-month fertility test. (B) Distribution of follicles at different developmental stages in ovaries treated with PBS (Ctrl) or HucMSC-exos (Exo). Primo, primordial follicle; Prima, primary follicle; Sec, secondary follicle; EA, early antral follicle; LA, late antral follicle; CL, corpus luteum. n = 5/group. (C) Number of mice that gave birth to pups during the test. (D) Comparison of the cumulative numbers of pups per female in the control group (blue) and HucMSC-exo-treated (red) group. Data are shown as mean ± SEM. *p < 0.05.

rapamycin. The results suggest that the two signaling pathways are both involved in the regulation of the effects of exos on primordial follicles. We previously demonstrated the synergistic stimulation of primordial follicles with the combined usage of PI3K and mTOR activators.[27] In this study, we propose that as an alternative to the traditional chemical stimulators of the signaling pathway, exos derived from MSCs may represent a new type of follicular activator that has the potential for future applications in the clinic.

Clinically, a significant reduction in the pool of primordial follicles is known as "diminished ovarian reserve" (DOR), which affects up to 10% of couples pursuing assisted reproduction.[47] In aging ovaries, DOR occurs as a normal part of human physiology, whereas in women with POI, the early exhaustion of ovarian follicles is evident together with amenorrhea, hypoestrogenism, and elevated gonadotropin levels before 40 years of age. Because of the arrest of spontaneous ovulation at an early age, the chances of POI patients conceiving are very low, and oocyte donation is normally recommended as the most efficient infertility treatment. Notably, residual dormant follicles are commonly found in POI ovaries. However, these follicles are difficult to grow via physiological processes. Our earlier studies have demonstrated the abilities of PI3K and mTOR stimulators to activate dormant murine and human primordial follicles *in vitro*.[27,48] The approach, which is named *in vitro* activation (IVA), enables POI patients to conceive using their own eggs after the ovarian cortex is activated *in vitro* and transplanted back into the body.[49] Until now, several successful pregnancies and live births after IVA treatment have been reported with the vitrified and fresh ovarian tissues of POI patients.[50,51] However, all of these cases were younger patients, and treatment success was determined by means of residual follicle numbers and the duration from POI diagnosis. It is well known that oocyte quality decreases with increasing maternal age, which is associated with an increased risk for miscarriage, aneuploidy in offspring, and even infertility.[5] Although IVA has the potential to promote follicle growth and increase oocyte numbers for POI treatment, it does not correct the age-related decline in egg quality.[52] However, our current study clearly demonstrated the rescue effects of HucMSC-exos treatment on the age-related retardation of oocyte production and oocyte quality. The restoration of mitochondrial functions was manifested as a significant decrease in ROS levels and a higher $\Delta\Psi m$ in HucMSC-exo-treated oocytes. MSCs have been shown to attenuate cigarette smoke medium-induced mitochondrial ROS and $\Delta\Psi m$ loss in airway cells by mitochondrial transfer and paracrine regulation.[53] MSCs from the umbilical cord were also found to reverse D-galactose-induced hepatic mitochondrial dysfunction via paracrine regulation of the Nrf2/HO-1 pathway.[54] Herein, in contrast to previous studies, our study provides new evidence that exo transfer may represent another way for MSCs to regulate mitochondrial functions in target cells.[55] Our results also suggest that exos derived from MSCs may be better IVA stimulators than traditional IVA chemicals, especially for women with age-related DOR.

Previously, the age-related decline in oocyte quality was thought to be due to the selection of the highest quality oocytes during the early reproductive years, leaving lower quality oocytes for the reproductive years of advanced age.[2] However, an increasing number of reports

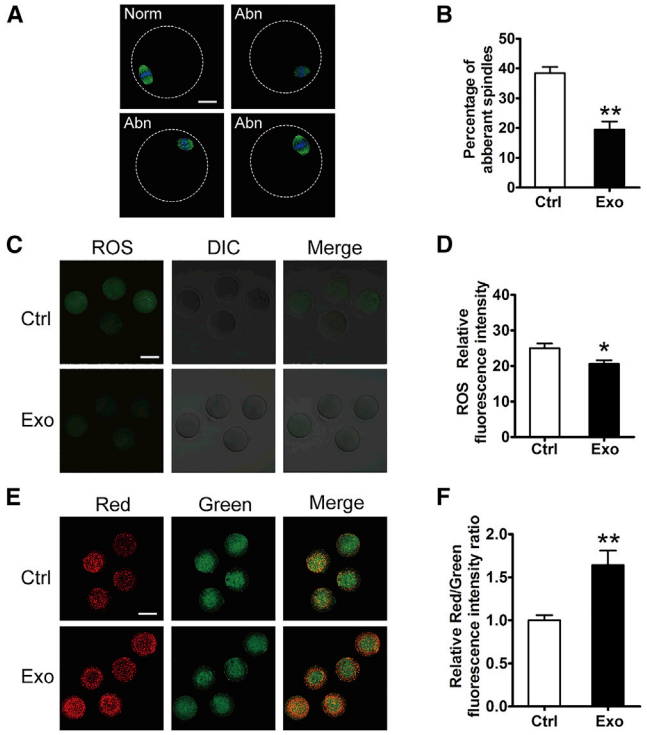

Figure 8. Evaluation of Oocyte Quality after HucMSC-exos Treatment *In Vivo*

Oocytes were collected from old mice by superovulation after a fertility test. (A) Representative morphology of MII oocytes with normal (Norm) or aberrant (Abn) spindles in PBS (Ctrl)- or HucMSC-Exo (Exo)-treated group. Green indicates β-tubulin; blue indicates nuclear staining with Hoechst 33342. (B) Percentage of aberrant oocytes in the two groups. n = 4 mice/group. (C and D) ROS fluorescence staining (green) (C) and relative fluorescence intensity ratio (D) in MII oocytes from control and HucMSC-exo-treated groups. Each group included 10 oocytes for analysis. (E) Oocyte mitochondrial membrane potential ($\Delta\Psi$m) shown by JC-1 staining between the two groups. Red indicates higher $\Delta\Psi$m; green indicates lower $\Delta\Psi$m. (F) The ratio of red/green fluorescence intensity reflects the increase in oocyte mitochondrial activity in HucMSC-exo-treated mice. *$p < 0.05$, **$p < 0.01$ compared with controls. Scale bars, 20 μm.

have revealed that the aging process itself exerts an unfavorable influence on the oocytes of dormant follicles before being selected in the ovulatory cohort.[6] The paracrine regulation of granulosa cell functions after treatment with MSCs or MSC-derived exos has been proposed in chemotherapy-induced POI animals.[12,22,23,56] The uptake of exos in equine or bovine granulosa cells was observed using both *in vitro* and *in vivo* methods.[57,58] However, until now, no one had determined whether the oocyte could internalize exos or the underlying mechanism. After culturing newborn ovaries with HucMSC-exos *in vitro*, we were surprised to find the specific enrichment of external exos in the oocytes of the primordial follicles. The primordial oocytes have always been thought to respond to signals only from contacts with surrounding pregranulosa cells.[59] Although we could not exclude the possibility that exo treatment improves granulosa cell functions and the ovarian microenvironment, our data at least revealed specific regulatory effects of HucMSC-exos on dormant oocytes and oocyte quality. Future studies will focus on whether oocytes with a zona pellucida in the developing follicles can also take up external exos. The mechanism of how exos are specifically enriched in primordial oocytes will be another interesting topic to be elucidated.

In summary, we demonstrated a new mechanism by which MSCs regulate the activation of dormant primordial follicles through the specific enrichment of secreted exos in oocytes. The increased recruitment of primordial follicles was related to the stimulatory effects of the exos on the oocyte PI3K and mTOR signaling pathways that functioned through the exo-carrying miRNAs, such as miR-146a-5p or miR-21-5p. The intrabursal injection of HucMSC-exos into old mice further demonstrated their rescuing effects on the age-related decrease in fertility, as shown by not only the increase in oocyte production but also the improvement in oocyte quality. However, exos from different sources of MSCs may comprise variable cargos, including inflammatory mediators, tropic factors, signaling molecules, mRNAs, miRNAs, and long non-coding RNAs (lncRNAs),[60] and it is worth determining whether exos from other MSC sources have similar effects on dormant oocytes. These types of studies will be beneficial toward identifying key exo-regulators that may function in oocytes. Because of the increasingly thorough studies of the superiority of MSC-derived exos as pharmaceutical entities with regard to efficacy, safety, and practicability, MSC-derived exos may be applied in the clinic as a surrogate IVA protocol, especially for women with age-related DOR.

MATERIALS AND METHODS

Experimental Animals

Mice were obtained from Vital River Laboratories (Beijing, China) and housed in the animal facility at Nanjing Medical University. Mice were maintained under a 12-h light/12-h dark cycle at 22°C with free access to food and water. All animal protocols were approved by the Committee on the Ethics of Animal Experiments at Nanjing Medical University. Ovaries of P2.5 ICR females were used for *in vitro* culture and transplanted into kidney capsules of the same strain of female mice at 8–10 weeks of age. Control oocytes for IVF were collected from P23 ICR female mice by superovulation, and adult male B6D2F1 mice (10–14 weeks old) were chosen as sperm donors. Female ICR mice at 10 months of age were used for intrabursal injection of HucMSC-exos, and the mating experiment was done with the same strain of adult male mice (8–10 weeks old).

Isolation and Culture of HucMSCs

Fresh umbilical cords were collected from informed, consenting mothers at the Sir Run Run Hospital of Nanjing Medical University. The experimental protocol was approved by the Ethics Committee of Nanjing Medical University. HucMSCs were isolated as previously described.[61] Briefly, tissues were washed with PBS (0.01 M [pH 7.4], HyClone, USA) containing 100 U/mL penicillin and 100 mg/mL streptomycin (Biofil, China) and cut into small pieces (1 mm^3). Tissues were plated in dishes and cultured in DMEM/F-12 (HyClone, USA) containing 10% fetal bovine serum (FBS; Gibco, USA) and 1% penicillin and streptomycin at 37°C and 5%

Please cite this article in press as: Yang et al., HucMSC-Derived Exosomes Mitigate the Age-Related Retardation of Fertility in Female Mice, Molecular Therapy (2020), https://doi.org/10.1016/j.ymthe.2020.02.003

CO_2. Culture medium was changed every 2 days until cells grew from cord tissues with 70%–80% adherence. The adherent cells were passaged with 0.25% trypsin-0.02% EDTA (Gibco, USA), and passage 3–7 MSCs were used to isolate exos. The phenotype profile of HucMSCs was evaluated through flow cytometry analysis by using antibodies against various markers, including positive markers CD44, CD73, CD90, and CD105 and negative markers CD11b, CD19, CD34, CD45, and human leukocyte antigen (HLA)-DR/DQ. All details of antibodies are shown in Table S1. MSC differentiation analyses were performed with passage 5 HucMSCs in HucMSC osteogenic (HUXUC-90021, Cyagen, USA), adipogenic (HUXUC-90031, Cyagen, USA), or chondrogenic differentiation medium (HUXUC-9004, Cyagen, USA) and differentiated cells were identified by alizarin red, oil red O, and Alcian blue.

Isolation and Characterization of HucMSC-exos

HucMSC-exos were isolated as previously described.[62] In brief, when cells reached 60%–70% confluence, culture medium was removed and washed with PBS three times. Cells were then cultured with exo-depleted conditioned medium for 48 h. Dead cells, cell debris, and large EVs were removed by a series of centrifugation at 500 × *g* (5814R, Eppendorf, Germany) for 10 min, 2,000 × *g* for 20 min, and 12,000 × *g* for 30 min. After filtration through a 0.22-μm syringe filter (SLGP033RB, Millipore, USA), the supernatants were ultracentrifuged (L-100XP, Beckman Coulter, USA) at 120,000 × *g* for 2 h by using a SW32Ti rotor to isolate exos. The pellets were then suspended in PBS and washed by ultracentrifugation at 120,000 × *g* for another 2 h. The produced exos were diluted in 150 μL of PBS. Particle size and concentrations were measured by NTA (Particle Metrix, Germany). All procedures were performed at 4°C.

TEM

Exo pellets obtained by ultracentrifugation were suspended and fixed in 100 μL of 2.5% glutaraldehyde overnight at 4°C. The fixed HucMSC-exos were dropped onto a carbon-coated copper grid and stained with 2% uranyl acetate for 2 min. After washing with ultrapure water, the grid was examined using a transmission electron microscope (Tecnai G2 Spirit BioTWIN, FEI, USA).

Uptake of HucMSC-exos by the Cultured Newborn Ovaries

Exo pellets obtained by ultracentrifugation were suspended with PKH67 green fluorescent labeling dye (Sigma, USA) at room temperature as instructed by the manufacturer, and then blocked by 1% BSA/PBS solution. Another 2 h of ultracentrifugation at 120,000 × *g* was applied to remove the un-conjugated dye. Labeled exos were then added into medium and incubated with P2.5 ovaries at different time intervals (3, 6, 12, and 24 h). 5,000 IU/mL heparin sodium (Sigma, USA) was used to prevent false-positive results. After treatment, ovaries were collected and fixed in 4% formaldehyde for frozen sections. After staining nuclei with 0.01 mg/mL Hoechst 33342 (Invitrogen, USA), the slides were observed and relative fluorescence intensity (PKH67, green) was calculated by using a confocal laser scanning microscope (LSM800, Zeiss, Germany).

In Vitro Ovarian Organ Culture and Ovarian Transplantation

P2.5 newborn ovaries were harvested and cultured on inserts (PICM01250, Millipore, USA) with 0.4 mL of culture medium added in the bottom of each well. The culture medium was minimum essential medium (MEM)-alpha supplemented with 0.23 mM pyruvic acid, 50 mg/L streptomycin sulfate, 75 mg/L penicillin G, 0.03 U/mL follicle-stimulating hormone (FSH), and 3 mg/mL BSA. Ovaries were randomly distributed to the control and treated groups, with each group containing three to four ovaries. Ovaries co-cultured with HucMSCs were used as positive controls. To see the time-dependent accumulation of HucMSC-exos, ovaries were cultured with PKH67-labeled exos for 3, 6, 12, and 24 h. To see the dose-dependent effects of HucMSC-exos, ovaries were treated for 24 h with HucMSC-exos that ranged from 5 to 20 μg/mL (3×10^8, 6×10^8, and 1.2×10^9 particles/mL, respectively). To determine the effects of inhibitors, ovaries were incubated with 20 μg/mL HucMSC-exos for 24 h with PI3K inhibitor LY294002 (20 μM), Akt inhibitor Akt VIII (5 μM, MCE, USA), mTOR inhibitor rapamycin (250 nM, Sigma, USA), and exo-internalization inhibitor heparin sodium (5,000 U/mL, Sigma, USA). In another experiment, after finishing the treatment, ovaries (n = 3–4) in each group were transferred to fresh control medium for another 96 h to evaluate follicular development. All control groups were added with equal volumes of PBS into the media. For the siRNA experiments, ovaries were pretreated with chemically modified mTOR siRNAs (5′-chol + 2′ OMe) and control (5′-chol + 2′ OMe + Cy3) siRNAs for 60 h. Ovaries were then transferred into control media and treated with or without HucMSC-exos for another 24 h to check the activation of the PI3K/mTOR signaling pathway. The mTOR siRNAs were synthesized by Ruibo Biotechnology (Guangzhou, China), and the oligonucleotide sequences were as follows: 5′-GAACTCGCTGATCCAGATG-3′ and 5′-GCGGATGGCT CCTGACTAT-3′.

For ovarian transplantation, paired ovaries were separated with one that served as a control and the other one being treated with 20 μg/mL HucMSC-exos for 24 h. After the treatment, paired ovaries were randomly inserted under either side of the kidney capsule of the same host. The hosts were ovariectomized and treated with 2 IU of FSH every 2 days. Some animals were sacrificed at 48 h or 4 days after transplantation to assess follicular development, some animals were sacrificed at 18 days to collect GV oocytes for IVM, and some animals were injected with 5 IU hCG (human chorionic gonadotrophin, Sansheng Biological Technology, China) at 18 days to collect MII mature oocytes 12 h later for IVF.

Isolation of Primordial Oocytes from Newborn Ovaries

Ovaries were harvested by carefully removing oviducts and ovarian bursa in calcium- and magnesium-free Hanks' balanced salt solution (HBSS, Invitrogen, USA) and then transferred to HBSS containing 0.25% trypsin, 1 mM ethylenediaminetetraacetic acid (EDTA), and 0.01% DNase I and incubated at 37°C for 8 min with gentle agitation. After removing the supernatant, ovaries were immediately washed twice with HBSS and transferred into DMEM/F-12 media

(Invitrogen, USA) supplemented with 0.05% collagenase IV (Sigma, USA) for 10 min with frequent pipetting until the tissues were completely dispersed. The mixture of cells and oocytes was then washed twice and cultured in a 6-cm tissue culture dish for 4 h to allow the somatic cells to attach to the plastic. The culture media containing unattached oocytes were then centrifuged for oocyte collection. The oocytes were resuspended in fresh DMEM/F-12 media supplemented with 3 mg/mL BSA (Sigma, USA), 100 U/mL penicillin, and 100 μg/mL streptomycin and starved for 12 h before treatment with HucMSC-exos with or without different PI3K or mTOR inhibitors. Oocytes in each group were collected for further analysis after 24 h of treatment.

IVM and IVF

For IVM studies, GV oocytes were harvested from grafted ovaries and cultured in M2 medium (Sigma, USA) under mineral oil (Sigma, USA) at 37°C in 5% CO_2. After 16 h of incubation, the MII mature oocytes/GV oocytes ratio was evaluated and MII oocytes were collected for morphology and immunofluorescence. For IVO studies, recipient mice at 18 days of transplantation were given a single injection of 5 IU of hCG and grafted ovaries were collected 14 h later into M2 medium containing 0.1% hyaluronidase (H3506, Sigma, USA). MII oocytes were directly obtained by mechanically puncturing with fine needles. Control GV and MII oocytes were collected from P25 ICR mice after superovulation with pregnant mare serum gonadotropin (PMSG) and hCG injections.

For IVF studies, donor sperm was collected from B6D2F1 male mice into human tubal fluid (HTF) media (MR-070-D, Millipore, USA) and incubated under oil for 1 h at 37°C in 5% CO_2 for capacitation. MII oocytes were then placed into 250 μL of media with sperm (2–3 × 105/mL) for 6–8 h. After fertilization, zygotes with clear pronuclei were transferred into fresh HTF media overnight until the two-cell embryonic stage. Two-cell embryos were then cultured in small droplets of KSOM media (MR-020P-5F, Millipore, USA) to blastocyst stage. Embryonic development was evaluated as the ratio of two-cell embryos to zygotes and the ratio of blastocysts to zygotes.

Intrabursal Injection and Fertility Test

After mice were anesthetized with tribromoethanol (Avertin; 240 mg/kg, Sigma, USA), two small incisions were made on the peritoneum to externalize the ovaries. A total volume of 20 μL of solution containing 10 μg of HucMSC-exos or PBS was prepared and injected through the fat pad into the ovarian bursa using a 31G insulin needle. For some animals, one lateral ovarian bursa was given exos and the other lateral bursa received PBS as control. Ovaries were collected 3 weeks later to evaluate follicular development. To perform fertility test experiments, HucMSC-exos or PBS were injected into bilateral ovarian bursas and were mated with the same strain of fertile males 3 weeks later. The mating trials lasted for 4 months. The number of offspring delivered per female was recorded once a week to plot a reproductive curve. At the end of the test, MII oocytes were obtained from mice in both groups with superovulation.

Immunoblotting Analysis

Ovarian proteins were extracted by radioimmunoprecipitation assay (RIPA) lysis buffer (P0013B, Beyotime Institute of Biotechnology) containing protease inhibitor cocktails (M221, Amresco). HucMSC-exos were dissolved in PBS and proteins were directly denatured with 5× loading buffer. A total of 10 or 30 μg of proteins in each sample was loaded and separated by electrophoresis (165-8000, Bio-Rad, USA). After electronic transfer (170-3930, Bio-Rad, USA), the polyvinylidene fluoride (PVDF) membranes (88250, Thermo Fisher Scientific, USA) were blocked in 20 mL of 5% milk for at least 1 h and then incubated overnight at 4°C with specific antibodies. Primary antibodies with respective dilutions (diluted to 1 mL) are listed in Table S1. After washing with Tris-buffered saline with Tween 20 (TBST) (5 mL) three times, the horseradish peroxidase (HRP)-conjugated relative secondary antibodies were then used to detect proteins through enhanced chemiluminescence (RPN2232, GE Healthcare, USA) on the Tanon 5200 analysis system.

Quantitative Real-Time PCR

Total RNAs of oocytes or ovaries were isolated by TRIzol reagent (Invitrogen, USA) according to the manufacturer's protocol. RNA concentrations were measured by a spectrophotometer (NanoDrop 2000c, Thermo Scientific, USA). 500 ng of RNA/reaction per sample was reverse transcribed using a FastQuant RT kit (Tiangen Biotech, China) to create cDNA. Quantitative real-time PCR was then performed using SYBR Green mix (Applied Biological Materials, Canada) on an ABI StepOnePlus platform (Thermo Scientific, USA). Quantification of various mRNAs was performed by using the actin amplification signal as the internal control. All of the primer sequences used are listed in Table S2. The specificity of the PCR products was assessed by melting curve analyses, and amplicon size was determined by electrophoresis in 2% agarose gels.

For ovarian miRNA detection, total RNA was first purified using an RNeasy micro kit (QIAGEN, Germany) and then for poly(A) tailing with a miDETECT A Track miRNA qRT-PCR start kit (RiboBio, Guangzhou, China). In brief, 1 μg of total RNA and 1 μL of poly(A) polymerase were heated at 37°C for 1 h. cDNA was synthesized at 42℃ for 1 h and then incubated at 72℃ for 10 min according to the kit's instruction. Quantitative real-time PCR was performed to quantify miRNAs with miDETECT A Track miRNA qRT-PCR primer sets (one RT primer and a pair of qPCR primers for each set) specific for miR-21-5p and miR-146a-5p designed by RiboBio (Guangzhou, China). All expression levels of miRNAs were normalized to U6.

Immunohistochemistry

Ovaries were collected and fixed in 10% buffered formalin for paraffin embedding and sectioning. To detect the expression and translocation of Foxo3a, 5-μm sections were deparaffinized, rehydrated, and endogenous peroxidase activity was blocked by incubation in 3% hydrogen peroxide in methanol for 15 min. The sections were then boiled in 0.01 M citrate buffer to retrieve the antigen. After blocking by goat serum (ZSGB-Bio, China) for 1 h, primary antibodies were

incubated overnight at 4°C, and diaminobenzidine (DAB) reagent was used for coloration on the second day. Non-immune immunoglobulin G (IgG) was applied as a negative control.

Follicle Counting

In vitro-cultured ovaries and ovaries from operated mice and intrabursally injected mice were collected and fixed in 10% buffered formalin overnight for serial sections (5 μm) and hematoxylin and eosin staining. To evaluate follicular development in operated and intrabursally injected mice, all follicles were counted at every fifth section using the fractionator and nucleator principles.[63] To evaluate the activation of primordial follicles, two serial sections from the largest cross-section through the center of each ovary were chosen for Foxo3a staining, and those primordial follicles with plasma translocate staining were counted as activated follicles.[64] All sections were counted by two independent individuals for comparison.

Immunofluorescence

MII oocytes from IVM, IVO, and superovulated mice were collected and the cumulus cells were removed by M2 medium containing 0.1% hyaluronidase. Oocytes were fixed in 4% paraformaldehyde for 30 min and then permeabilized with 0.5% Triton X-100 (Sigma-Aldrich, USA) for 20 min at room temperature. After blocking in 1% BSA/PBS solution for 1 h, oocytes were incubated with anti-β-tubulin antibody overnight at 4°C. After washing in 1% BSA/PBS, oocytes were incubated with Alexa Fluor 488 goat anti-rabbit secondary antibody (Invitrogen, Carlsbad, CA, USA) for 40 min at room temperature. The nuclei were then counterstained with 0.01 mg/mL Hoechst 33342 (Invitrogen, USA) for 15 min. All oocytes were put on the slides and observed by confocal microscopy (LSM700, Zeiss, Germany).

Exosomal miRNA Interference

Antagonists of miRNAs, Antagomir-146a-5p and Antagomir-21-5p (micrOFF miRNA Antagomir; RiboBio, Guangzhou, China), were transfected into HucMSC-exos by Lipofectamine 2000 (Invitrogen, Waltham, MA, USA) according to the instructions of the manufacturer. Briefly, the exo pellets isolated from 200 mL of conditioned media were resuspended with 100 μL of PBS containing 100 nM Antagomir plus 2 μL of Lipofectamine 2000 and incubated at 37°C for 4 h. After washing with PBS, Antagomir-containing exos were pelleted by ultracentrifugation at 120,000 × *g* for 2 h. Finally, 150 μL of PBS was added to resuspend the pellet, and same concentrations of HucMSC-exos and Antagomir-containing exos (20 μg/mL) were used for ovarian treatment. In some cases, Antagomirs or miRNA mimics, Agomir-146a-5p and Agomir-21-5p (micrON miRNA agomir; RiboBio, Guangzhou, China), were also incubated with cultured ovaries as controls. To better elucidate the specificity of HucMSCs carrying exos, we used paired ovaries and separated the pair for different treatments: Exo versus ExoKd1 (Exo containing Antagomir-146a-5p); Exo versus ExoKd2 (Exo containing Antagomir-21-5p); Exo versus Exo KdMix; ExoKd1 versus ExoKd1+Ago 146 (Agomir-146-5p); Ctrl versus Anta 146 (Antagomir-146a-5p); and Crtl versus Ago 146 (Agomir-146a-5p).

ROS and ΔΨm Measurement

To determine the ROS content and ΔΨm in oocytes, the procedure was conducted according to the instructions with the ROS kit (50101ES01, Yeasen, China) and the JC-1 ΔΨm assay kit (40706ES60, Yeasen, China). Briefly, the collected MII oocytes were washed with M2 medium several times and then transferred into M2 medium containing staining solution and incubated at 37°C in the dark for 30 min. After that, oocytes were washed with M2 medium to remove the excess staining solution. All of the live oocytes were observed, and relative fluorescence intensity was calculated by confocal microscopy (LSM700, Zeiss, Germany).

Statistical Analysis

GraphPad Prism 6.0 and SPSS 20.0 were used to perform the chi-square test, or one-way ANOVA and a Mann-Whitney U test to evaluate differences between groups. Data are shown as mean ± SEM. $p < 0.05$ was considered to be statistically significant.

SUPPLEMENTAL INFORMATION

Supplemental Information can be found online at https://doi.org/10.1016/j.ymthe.2020.02.003.

AUTHOR CONTRIBUTIONS

J.L., B.X., and T.W. conceptualized the study. W.Y., J.Z., and J.L. led the experimental design and wrote the manuscript. W.Y, J.Z., J.L., B.X., W.L., and Y.H. performed the experiments. S.Z., X.L., D.S., and T.W. provided human samples and corrected the manuscript. All authors analyzed and interpreted the data.

CONFLICTS OF INTEREST

The authors declare no competing interests.

ACKNOWLEDGMENTS

We would like to thank Prof. Jun Gao and Dr. Tian Tian at Nanjing Medical University for advice on our experimental design and for help on isolation and identification of exosomes. This work was supported by the National Key Research and Development Program of China (2018YFC1003703, 2018YFC1004203), the National Natural Science Foundation of China (31871513, 31671202), and the Nanjing Medical University Science and Technology Development Fund (2016NJMUZD018).

REFERENCES

1. Skinner, M.K. (2005). Regulation of primordial follicle assembly and development. Hum. Reprod. Update *11*, 461–471.
2. McLaughlin, E.A., and McIver, S.C. (2009). Awakening the oocyte: controlling primordial follicle development. Reproduction *137*, 1–11.
3. Reddy, P., Zheng, W., and Liu, K. (2010). Mechanisms maintaining the dormancy and survival of mammalian primordial follicles. Trends Endocrinol. Metab. *21*, 96–103.
4. Macklon, N.S., and Fauser, B.C. (1999). Aspects of ovarian follicle development throughout life. Horm. Res. *52*, 161–170.
5. Broekmans, F.J., Soules, M.R., and Fauser, B.C. (2009). Ovarian aging: mechanisms and clinical consequences. Endocr. Rev. *30*, 465–493.

6. Nelson, S.M., Telfer, E.E., and Anderson, R.A. (2013). The ageing ovary and uterus: new biological insights. Hum. Reprod. Update *19*, 67–83.
7. Qiao, J., Wang, Z.B., Feng, H.L., Miao, Y.L., Wang, Q., Yu, Y., Wei, Y.C., Yan, J., Wang, W.H., Shen, W., et al. (2014). The root of reduced fertility in aged women and possible therapentic options: current status and future perspects. Mol. Aspects Med. *38*, 54–85.
8. Podfigurna-Stopa, A., Czyzyk, A., Grymowicz, M., Smolarczyk, R., Katulski, K., Czajkowski, K., and Meczekalski, B. (2016). Premature ovarian insufficiency: the context of long-term effects. J. Endocrinol. Invest. *39*, 983–990.
9. Phinney, D.G., and Prockop, D.J. (2007). Concise review: mesenchymal stem/multipotent stromal cells: the state of transdifferentiation and modes of tissue repair—current views. Stem Cells *25*, 2896–2902.
10. Ding, D.C., Chang, Y.H., Shyu, W.C., and Lin, S.Z. (2015). Human umbilical cord mesenchymal stem cells: a new era for stem cell therapy. Cell Transplant. *24*, 339–347.
11. Li, T., Xia, M., Gao, Y., Chen, Y., and Xu, Y. (2015). Human umbilical cord mesenchymal stem cells: an overview of their potential in cell-based therapy. Expert Opin. Biol. Ther. *15*, 1293–1306.
12. Sheikhansari, G., Aghebati-Maleki, L., Nouri, M., Jadidi-Niaragh, F., and Yousefi, M. (2018). Current approaches for the treatment of premature ovarian failure with stem cell therapy. Biomed. Pharmacother. *102*, 254–262.
13. Li, J., Mao, Q., He, J., She, H., Zhang, Z., and Yin, C. (2017). Human umbilical cord mesenchymal stem cells improve the reserve function of perimenopausal ovary via a paracrine mechanism. Stem Cell Res. Ther. *8*, 55.
14. Ding, C., Zou, Q., Wang, F., Wu, H., Chen, R., Lv, J., Ling, M., Sun, J., Wang, W., Li, H., and Huang, B. (2018). Human amniotic mesenchymal stem cells improve ovarian function in natural aging through secreting hepatocyte growth factor and epidermal growth factor. Stem Cell Res. Ther. *9*, 55.
15. Ding, L., Yan, G., Wang, B., Xu, L., Gu, Y., Ru, T., Cui, X., Lei, L., Liu, J., Sheng, X., et al. (2018). Transplantation of UC-MSCs on collagen scaffold activates follicles in dormant ovaries of POF patients with long history of infertility. Sci. China Life Sci. *61*, 1554–1565.
16. Lai, R.C., Yeo, R.W., and Lim, S.K. (2015). Mesenchymal stem cell exosomes. Semin. Cell Dev. Biol. *40*, 82–88.
17. Basu, J., and Ludlow, J.W. (2016). Exosomes for repair, regeneration and rejuvenation. Expert Opin. Biol. Ther. *16*, 489–506.
18. Tkach, M., and Théry, C. (2016). Communication by extracellular vesicles: where we are and where we need to go. Cell *164*, 1226–1232.
19. Hu, Y., Rao, S.S., Wang, Z.X., Cao, J., Tan, Y.J., Luo, J., Li, H.M., Zhang, W.S., Chen, C.Y., and Xie, H. (2018). Exosomes from human umbilical cord blood accelerate cutaneous wound healing through miR-21-3p-mediated promotion of angiogenesis and fibroblast function. Theranostics *8*, 169–184.
20. Rani, S., Ryan, A.E., Griffin, M.D., and Ritter, T. (2015). Mesenchymal stem cell-derived extracellular vesicles: toward cell-free therapeutic applications. Mol. Ther. *23*, 812–823.
21. Reiner, A.T., Witwer, K.W., van Balkom, B.W.M., de Beer, J., Brodie, C., Corteling, R.L., Gabrielsson, S., Gimona, M., Ibrahim, A.G., de Kleijn, D., et al. (2017). Concise review: developing best-practice models for the therapeutic use of extracellular vesicles. Stem Cells Transl. Med. *6*, 1730–1739.
22. Xiao, G.Y., Cheng, C.C., Chiang, Y.S., Cheng, W.T., Liu, I.H., and Wu, S.C. (2016). Exosomal miR-10a derived from amniotic fluid stem cells preserves ovarian follicles after chemotherapy. Sci. Rep. *6*, 23120.
23. Huang, B., Lu, J., Ding, C., Zou, Q., Wang, W., and Li, H. (2018). Exosomes derived from human adipose mesenchymal stem cells improve ovary function of premature ovarian insufficiency by targeting SMAD. Stem Cell Res. Ther. *9*, 216.
24. Cheng, L., Sun, X., Scicluna, B.J., Coleman, B.M., and Hill, A.F. (2014). Characterization and deep sequencing analysis of exosomal and non-exosomal miRNA in human urine. Kidney Int. *86*, 433–444.
25. Li, J., Kawamura, K., Cheng, Y., Liu, S., Klein, C., Liu, S., Duan, E.K., and Hsueh, A.J. (2010). Activation of dormant ovarian follicles to generate mature eggs. Proc. Natl. Acad. Sci. USA *107*, 10280–10284.
26. Atai, N.A., Balaj, L., van Veen, H., Breakefield, X.O., Jarzyna, P.A., Van Noorden, C.J., Skog, J., and Maguire, C.A. (2013). Heparin blocks transfer of extracellular vesicles between donor and recipient cells. J. Neurooncol. *115*, 343–351.
27. Sun, X., Su, Y., He, Y., Zhang, J., Liu, W., Zhang, H., Hou, Z., Liu, J., and Li, J. (2015). New strategy for in vitro activation of primordial follicles with mTOR and PI3K stimulators. Cell Cycle *14*, 721–731.
28. Dou, X., Sun, Y., Li, J., Zhang, J., Hao, D., Liu, W., Wu, R., Kong, F., Peng, X., and Li, J. (2017). Short-term rapamycin treatment increases ovarian lifespan in young and middle-aged female mice. Aging Cell *16*, 825–836.
29. Simon, A.M., Goodenough, D.A., Li, E., and Paul, D.L. (1997). Female infertility in mice lacking connexin 37. Nature *385*, 525–529.
30. Kourembanas, S. (2015). Exosomes: vehicles of intercellular signaling, biomarkers, and vectors of cell therapy. Annu. Rev. Physiol. *77*, 13–27.
31. Bagno, L., Hatzistergos, K.E., Balkan, W., and Hare, J.M. (2018). Mesenchymal stem cell-based therapy for cardiovascular disease: progress and challenges. Mol. Ther. *26*, 1610–1623.
32. Zhu, Z., Zhang, Y., Zhang, Y., Zhang, H., Liu, W., Zhang, N., Zhang, X., Zhou, G., Wu, L., Hua, K., and Ding, J. (2019). Exosomes derived from human umbilical cord mesenchymal stem cells accelerate growth of VK2 vaginal epithelial cells through microRNAs in vitro. Hum. Reprod. *34*, 248–260.
33. Sun, X., Cui, S., Fu, X., Liu, C., Wang, Z., and Liu, Y. (2019). MicroRNA-146-5p promotes proliferation, migration and invasion in lung cancer cells by targeting claudin-12. Cancer Biomark. *25*, 89–99.
34. Fu, X., He, Y., Wang, X., Peng, D., Chen, X., Li, X., and Wang, Q. (2017). Overexpression of miR-21 in stem cells improves ovarian structure and function in rats with chemotherapy-induced ovarian damage by targeting PDCD4 and PTEN to inhibit granulosa cell apoptosis. Stem Cell Res. Ther. *8*, 187.
35. May-Panloup, P., Boucret, L., Chao de la Barca, J.M., Desquiret-Dumas, V., Ferré-L'Hotellier, V., Morinière, C., Descamps, P., Procaccio, V., and Reynier, P. (2016). Ovarian ageing: the role of mitochondria in oocytes and follicles. Hum. Reprod. Update *22*, 725–743.
36. Wilding, M., Dale, B., Marino, M., di Matteo, L., Alviggi, C., Pisaturo, M.L., Lombardi, L., and De Placido, G. (2001). Mitochondrial aggregation patterns and activity in human oocytes and preimplantation embryos. Hum. Reprod. *16*, 909–917.
37. Takahashi, T., Takahashi, E., Igarashi, H., Tezuka, N., and Kurachi, H. (2003). Impact of oxidative stress in aged mouse oocytes on calcium oscillations at fertilization. Mol. Reprod. Dev. *66*, 143–152.
38. Colao, I.L., Corteling, R., Bracewell, D., and Wall, I. (2018). Manufacturing exosomes: a promising therapeutic platform. Trends Mol. Med. *24*, 242–256.
39. Doeppner, T.R., Herz, J., Görgens, A., Schlechter, J., Ludwig, A.K., Radtke, S., de Miroschedji, K., Horn, P.A., Giebel, B., and Hermann, D.M. (2015). Extracellular vesicles improve post-stroke neuroregeneration and prevent postischemic immunosuppression. Stem Cells Transl. Med. *4*, 1131–1143.
40. Kim, D.K., Nishida, H., An, S.Y., Shetty, A.K., Bartosh, T.J., and Prockop, D.J. (2016). Chromatographically isolated $CD63^{+}CD81^{+}$ extracellular vesicles from mesenchymal stromal cells rescue cognitive impairments after TBI. Proc. Natl. Acad. Sci. USA *113*, 170–175.
41. Lee, C., Mitsialis, S.A., Aslam, M., Vitali, S.H., Vergadi, E., Konstantinou, G., Sdrimas, K., Fernandez-Gonzalez, A., and Kourembanas, S. (2012). Exosomes mediate the cytoprotective action of mesenchymal stromal cells on hypoxia-induced pulmonary hypertension. Circulation *126*, 2601–2611.
42. Zhang, J., Guan, J., Niu, X., Hu, G., Guo, S., Li, Q., Xie, Z., Zhang, C., and Wang, Y. (2015). Exosomes released from human induced pluripotent stem cells-derived MSCs facilitate cutaneous wound healing by promoting collagen synthesis and angiogenesis. J. Transl. Med. *13*, 49.
43. Adhikari, D., and Liu, K. (2009). Molecular mechanisms underlying the activation of mammalian primordial follicles. Endocr. Rev. *30*, 438–464.
44. Castrillon, D.H., Miao, L., Kollipara, R., Horner, J.W., and DePinho, R.A. (2003). Suppression of ovarian follicle activation in mice by the transcription factor Foxo3a. Science *301*, 215–218.

45. Reddy, P., Liu, L., Adhikari, D., Jagarlamudi, K., Rajareddy, S., Shen, Y., Du, C., Tang, W., Hämäläinen, T., Peng, S.L., et al. (2008). Oocyte-specific deletion of *Pten* causes premature activation of the primordial follicle pool. Science *319*, 611–613.

46. Adhikari, D., Zheng, W., Shen, Y., Gorre, N., Hämäläinen, T., Cooney, A.J., Huhtaniemi, I., Lan, Z.J., and Liu, K. (2010). Tsc/mTORC1 signaling in oocytes governs the quiescence and activation of primordial follicles. Hum. Mol. Genet. *19*, 397–410.

47. Yin, O., Cayton, K., and Segars, J.H. (2016). In vitro activation: a dip into the primordial follicle pool? J. Clin. Endocrinol. Metab. *101*, 3568–3570.

48. Lo, B.K.M., Sheikh, S., and Williams, S.A. (2019). In vitro and in vivo mouse follicle development in ovaries and reaggregated ovaries. Reproduction *157*, 135–148.

49. Kawamura, K., Cheng, Y., Suzuki, N., Deguchi, M., Sato, Y., Takae, S., Ho, C.H., Kawamura, N., Tamura, M., Hashimoto, S., et al. (2013). Hippo signaling disruption and Akt stimulation of ovarian follicles for infertility treatment. Proc. Natl. Acad. Sci. USA *110*, 17474–17479.

50. Kawamura, K., Cheng, Y., Sun, Y.P., Zhai, J., Diaz-Garcia, C., Simon, C., Pellicer, A., and Hsueh, A.J. (2015). Ovary transplantation: to activate or not to activate. Hum. Reprod. *30*, 2457–2460.

51. Zhai, J., Yao, G., Dong, F., Bu, Z., Cheng, Y., Sato, Y., Hu, L., Zhang, Y., Wang, J., Dai, S., et al. (2016). In vitro activation of follicles and fresh tissue auto-transplantation in primary ovarian insufficiency patients. J. Clin. Endocrinol. Metab. *101*, 4405–4412.

52. Suzuki, N., Yoshioka, N., Takae, S., Sugishita, Y., Tamura, M., Hashimoto, S., Morimoto, Y., and Kawamura, K. (2015). Successful fertility preservation following ovarian tissue vitrification in patients with primary ovarian insufficiency. Hum. Reprod. *30*, 608–615.

53. Li, X., Michaeloudes, C., Zhang, Y., Wiegman, C.H., Adcock, I.M., Lian, Q., Mak, J.C.W., Bhavsar, P.K., and Chung, K.F. (2018). Mesenchymal stem cells alleviate oxidative stress-induced mitochondrial dysfunction in the airways. J. Allergy Clin. Immunol. *141*, 1634–1645.e5.

54. Yan, W., Li, D., Chen, T., Tian, G., Zhou, P., and Ju, X. (2017). Umbilical cord MSCs reverse D-galactose-induced hepatic mitochondrial dysfunction via activation of Nrf2/HO-1 pathway. Biol. Pharm. Bull. *40*, 1174–1182.

55. Spees, J.L., Lee, R.H., and Gregory, C.A. (2016). Mechanisms of mesenchymal stem/stromal cell function. Stem Cell Res. Ther. *7*, 125.

56. Zhang, Q., Sun, J., Huang, Y., Bu, S., Guo, Y., Gu, T., Li, B., Wang, C., and Lai, D. (2019). Human amniotic epithelial cell-derived exosomes restore ovarian function by transferring microRNAs against apoptosis. Mol. Ther. Nucleic Acids *16*, 407–418.

57. Hung, W.T., Navakanitworakul, R., Khan, T., Zhang, P., Davis, J.S., McGinnis, L.K., and Christenson, L.K. (2017). Stage-specific follicular extracellular vesicle uptake and regulation of bovine granulosa cell proliferation. Biol. Reprod. *97*, 644–655.

58. da Silveira, J.C., Veeramachaneni, D.N., Winger, Q.A., Carnevale, E.M., and Bouma, G.J. (2012). Cell-secreted vesicles in equine ovarian follicular fluid contain miRNAs and proteins: a possible new form of cell communication within the ovarian follicle. Biol. Reprod. *86*, 71.

59. Clarke, H.J. (2018). Regulation of germ cell development by intercellular signaling in the mammalian ovarian follicle. Wiley Interdiscip. Rev. Dev. Biol. *7*.

60. Ren, K. (2019). Exosomes in perspective: a potential surrogate for stem cell therapy. Odontology *107*, 271–284.

61. Qiao, C., Xu, W., Zhu, W., Hu, J., Qian, H., Yin, Q., Jiang, R., Yan, Y., Mao, F., Yang, H., et al. (2008). Human mesenchymal stem cells isolated from the umbilical cord. Cell Biol. Int. *32*, 8–15.

62. Hoshino, A., Costa-Silva, B., Shen, T.L., Rodrigues, G., Hashimoto, A., Tesic Mark, M., Molina, H., Kohsaka, S., Di Giannatale, A., Ceder, S., et al. (2015). Tumour exosome integrins determine organotropic metastasis. Nature *527*, 329–335.

63. Flaws, J.A., Abbud, R., Mann, R.J., Nilson, J.H., and Hirshfield, A.N. (1997). Chronically elevated luteinizing hormone depletes primordial follicles in the mouse ovary. Biol. Reprod. *57*, 1233–1237.

64. He, Y., Peng, X., Wu, T., Yang, W., Liu, W., Zhang, J., Su, Y., Kong, F., Dou, X., and Li, J. (2017). Restricting the induction of NGF in ovarian stroma engenders selective follicular activation through the mTOR signaling pathway. Cell Death Dis. *8*, e2817.

YMTHE, Volume *28*

Supplemental Information

HucMSC-Derived Exosomes Mitigate the Age-Related Retardation of Fertility in Female Mice

Weijie Yang, Jing Zhang, Boqun Xu, Yuanlin He, Wei Liu, Jiazhao Li, Songying Zhang, Xiaona Lin, Dongming Su, Tinghe Wu, and Jing Li

Supplementary Figure Legend

Figure S1. Specific effects of HucMSC-exos on follicular activation and development. (A) Western blot showing the expressions of p-Akt (Ser473), p-mTOR (Ser2448), p-rpS6 (Ser235/236) in ovaries treated with or without HucMSC-exos for 24 h. Ovaries co-cultured with HucMSC were used as positive control. The expressions of Akt, mTOR, rpS6, and β-actin were used as internal controls. Ctrl, PBS; Exo, HucMSC-exos 20 μg/mL; MSC, HucMSC. (B) Western blot of the expression of p-Akt (Ser473), p-mTOR (Ser2448), p-rpS6 (Ser235/236) in isolated primordial oocytes treated with HucMSC-exos with/without Akt inhibitor, Akt VIII (AI) and mTOR inhibitor, rapamycin (Ra) for 24 h. (C and D) Blocking effects of mTOR knockdown on HucMSC-exos induced activation of PI3K/mTOR signaling pathway. Newborn ovaries were pretreated with mTOR siRNAs for 60 h, following with 24 h of treatment with or without HucMSC-exos. RT-PCR showing the effective knockdown of mTOR mRNAs (C); Western blot showing the decreased expression of p-Akt (Ser473), mTOR and p-mTOR (Ser2448), p-rpS6 (Ser235/236) in treated newborn ovaries (D). The expressions of Akt, rpS6, and β-actin were used as internal controls. siNC, control siRNA; siNC+E, control siRNA+HucMSC-exos; siM, mTOR siRNAs; siM+E, mTOR siRNAs+HucMSC-exos. (E) TUNEL assay of apoptosis in ovaries treated with or without HucMSC-exos. Paired ovaries were separated and treated with or without HucMSC-exos for 24 h and transplanted under kidney capsules of the same recipient mice. Ovaries were collected 48 h after transplantation. Green, TUNEL positive cells; Blue, nuclear staining with Hoechst 33342. Bar=20 μm. (F) Ovarian PCNA staining in nuclei of oocytes and granulosa cells. Bar=50 μm.

Figure S2. Histology of follicular development between paired ovaries treated with or without HucMSC-exos. Mice at 10 month of age were intra-bursa injected with 20 μL HucMSC-exos in one lateral ovary and same volume of PBS in the other lateral ovary. Paired ovaries were collected 3 weeks later for morphological analysis. Representative three pairs of ovaries were shown. In each group, right panels are magnifications of left panels. Bar=50μm.

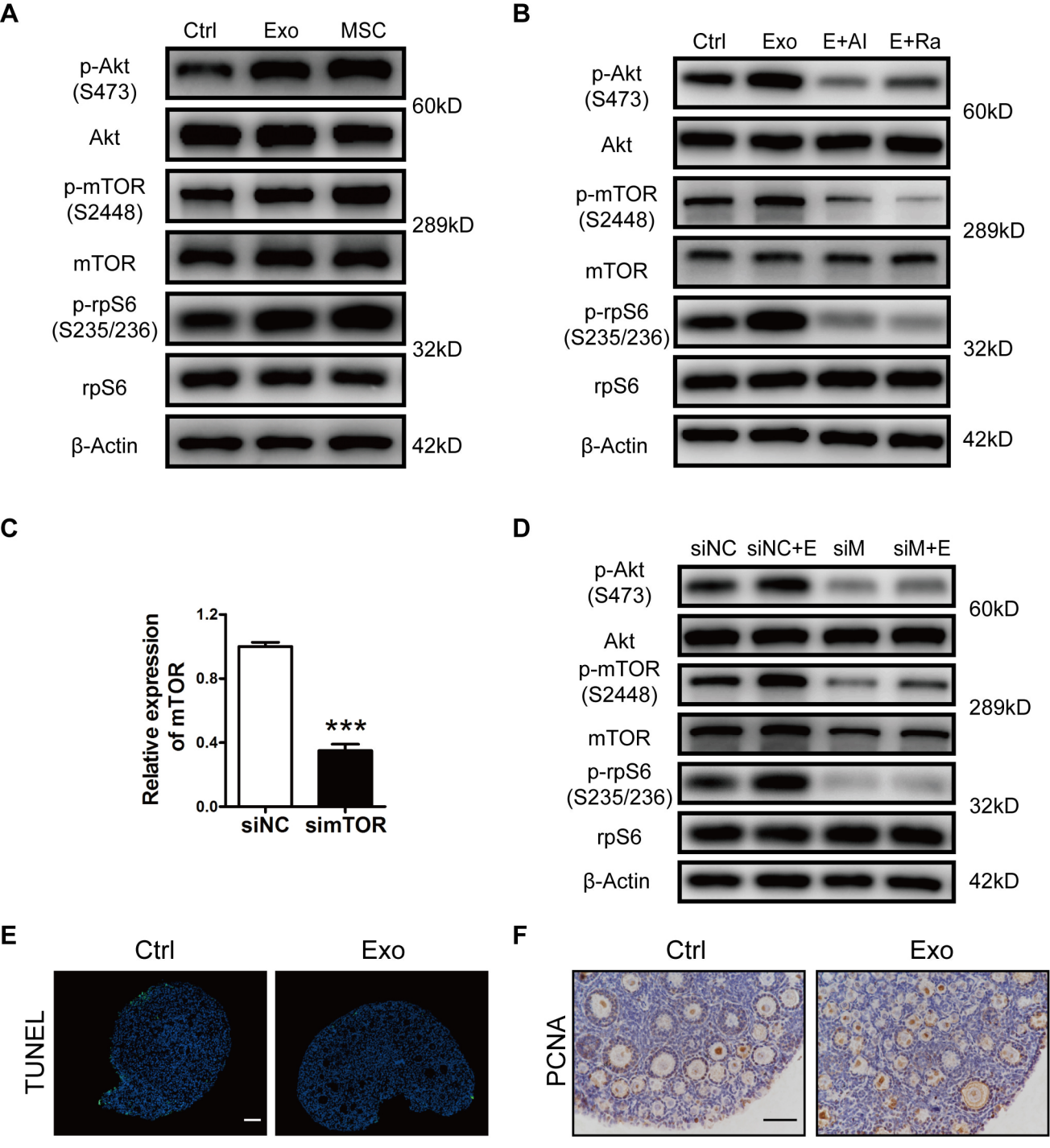
A
Ctrl
Exo
MSC
p-Akt (S473)
Akt
p-mTOR (S2448)
mTOR
p-rpS6 (S235/236)
rpS6
β-Actin
60kD
289kD
32kD
42kD
B
Ctrl
Exo
E+AI
E+Ra
p-Akt (S473)
Akt
p-mTOR (S2448)
mTOR
p-rpS6 (S235/236)
rpS6
β-Actin
60kD
289kD
32kD
42kD
C
Relative expression of mTOR
1.2
0.8
0.4
0.0
***
siNC
simTOR
D
siNC
siNC+E
siM
siM+E
p-Akt (S473)
Akt
p-mTOR (S2448)
mTOR
p-rpS6 (S235/236)
rpS6
β-Actin
60kD
289kD
32kD
42kD
E
Ctrl
Exo
TUNEL
F
Ctrl
Exo
PCNA

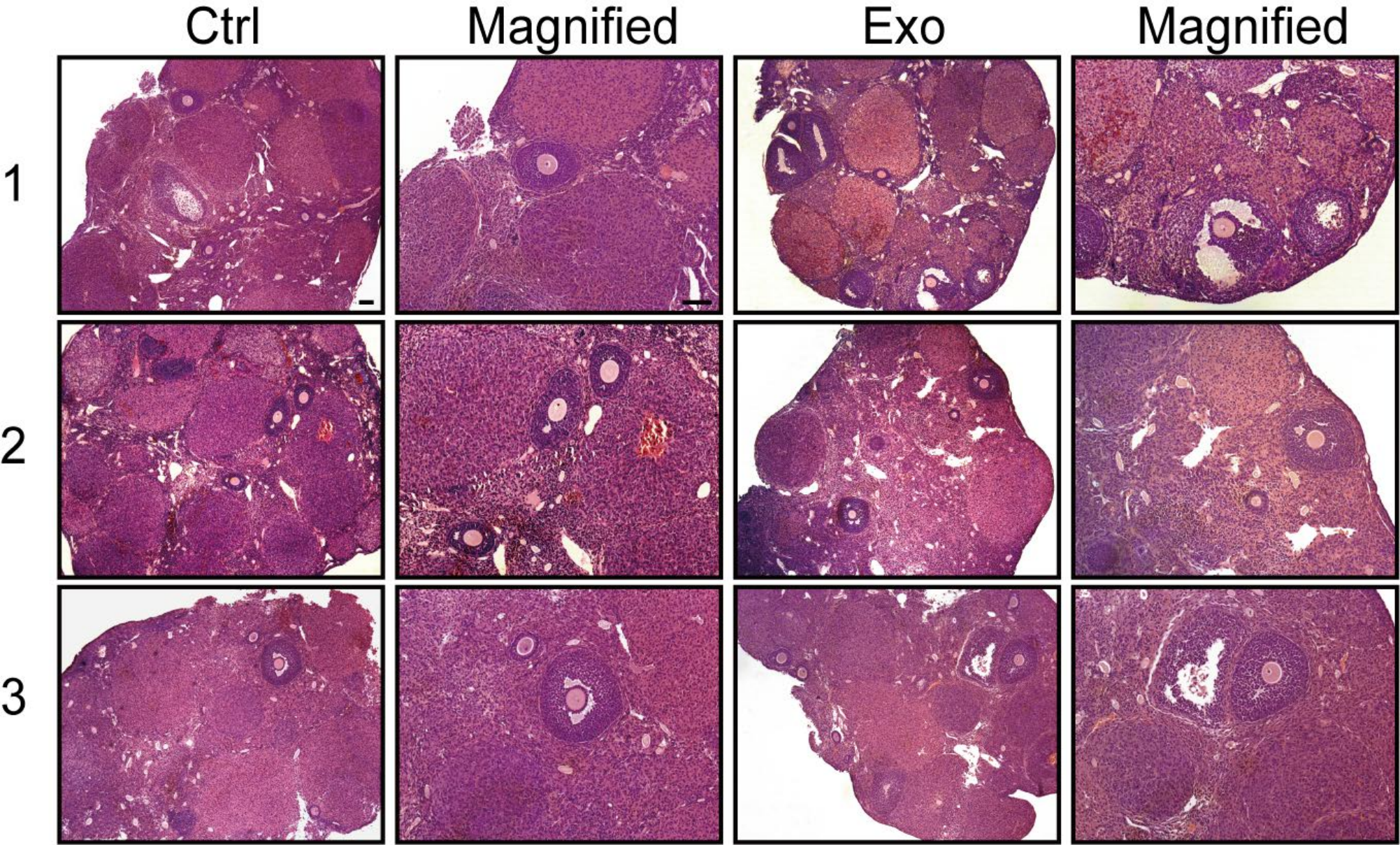
Ctrl
Magnified
Exo
Magnified
1
2
3

Supplementary Table S1

Antibody	Company	Catalog Number	Dilution
PE-conjugatedCD11b Antibody	BD	561689	1 test/10^6 cells
FITC-conjugatedCD19 Antibody	BD	560994	1 test/10^6 cells
FITC-conjugatedCD34 Antibody	BD	560942	1 test/10^6 cells
FITC-conjugatedCD44 Antibody	BD	560977	1 test/10^6 cells
FITC-conjugatedCD45 Antibody	BD	560976	1 test/10^6 cells
PE-conjugatedCD73 Antibody	BD	561014	1 test/10^6 cells
PE-conjugatedCD90 Antibody	BD	561970	1 test/10^6 cells
APC-conjugatedCD105 Antibody	BD	562408	1 test/10^6 cells
FITC-conjugatedHLA-DR/DQ Antibody	BD	555563	1 test/10^6 cells
β-Actin Antibody	CST	3700	WB 1:2000
GAPDH Antibody	CST	5174	WB 1:2000
Alix Antibody	Proteintech	12422-1-AP	WB 1:1000
Tsg101 Antibody	Abclonal	A2216	WB 1:1000
CD9 Antibody	Proteintech	20597-1-AP	WB 1:1000
Gm130 Antibody	BD	610822	WB 1:1000
rpS6 Antibody	CST	2217	WB 1:1000
p-rpS6（S235/236）Antibody	CST	2211	WB 1:1000
mTOR Antibody	CST	2983	WB 1:1000
p-mTOR Antibody	CST	5536	WB 1:1000
AKT Antibody	CST	2920	WB 1:1000
p-AKT Antibody	CST	4060	WB 1:1000
Foxo3a Antibody	CST	12829	IHC 1:200
PCNA Antibody	CST	13110	IHC 1:1000
Cx37 Antibody	Abcam	Ab181701	IF 1:200 WB 1:1000

Supplementary Table S2 Real-time PCR Primers

Gene	Forward primer	Reverse primer
Actin	5’-CCGTAAAGACCTCTATGCC-3′	5′-CTCAGTAACAGTCCGCCTA-3′
Gdf9	5′-TCTTAGTAGCCTTAGCTCTCAGG-3′	5′-TGTCAGTCCCATCTACAGGCA-3′
Zp3	5′-CATCTCAAAGTCGCGCCAG-3′	5′-GCCTGCGGTTTCGAGAAAC-3′
Bmp15	5′-TCCTTGCTGACGACCCTACAT-3′	5′-TACCTCAGGGGATAGCCTTGG-3′
Amhr	5′-GCAGCACAAGTATCCCCAAAC-3′	5′-GTCTCGGCATCCTTGCATCTC-3′
Kit	5′-CTCCCCCAACAGTGTATTCAC-3′	5′-TAGCCCGAAATCGCAAATCTT-3′
Kitl	5′-GAATCTCCGAAGAGGCCAGAA-3′	5′-GCTGCAACAGGGGGTAACAT-3′
Fshr	5′-CCTTGCTCCTGGTCTCCTTG-3′	5′-CTCGGTCACCTTGCTATCTTG-3′
Star	5′-ATGTTCCTCGCTACGTTCAAG-3′	5′-CCCAGTGCTCTCCAGTTGAG-3′